

UNCLASSIFIED

AD NUMBER

ADB004286

LIMITATION CHANGES

TO:

Approved for public release; distribution is unlimited.

FROM:

Distribution authorized to U.S. Gov't. agencies only; Test and Evaluation; FEB 1975. Other requests shall be referred to Air Force Avionics Lab., Wright-Patterson AFB, OH 45433.

AUTHORITY

AFAL ltr 19 Oct 1981

THIS PAGE IS UNCLASSIFIED

**THIS REPORT HAS BEEN DELIMITED
AND CLEARED FOR PUBLIC RELEASE
UNDER DOD DIRECTIVE 5200.20 AND
NO RESTRICTIONS ARE IMPOSED UPON
ITS USE AND DISCLOSURE.**

DISTRIBUTION STATEMENT A

**APPROVED FOR PUBLIC RELEASE,
DISTRIBUTION UNLIMITED.**

L
AFAL-TR-75-4

AD B 004286

200 WATT COMPACT CO₂ LASER

**GTE SYLVANIA INC.
ELECTRO-OPTICS ORGANIZATION
MOUNTAIN VIEW, CALIFORNIA**

TECHNICAL REPORT AFAL-TR-75-4

FEBRUARY 1975

FINAL REPORT FOR PERIOD NOVEMBER 1973 — DECEMBER 1974

Distribution limited to U.S. Government agencies only; test and evaluation results reported; (February 1975). Other requests for this document must be referred to the Air Force Avionics Laboratory (AFAL/TEO), Wright-Patterson AFB, Ohio 45433.

**AIR FORCE AVIONICS LABORATORY
AIR FORCE SYSTEMS COMMAND
WRIGHT-PATTERSON AIR FORCE BASE, OHIO 45433**

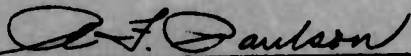


NOTICE

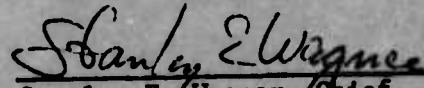
When Government drawings, specifications, or other data are used for any purpose other than in connection with a definitely related Government procurement operation, the United States Government thereby incurs no responsibility nor any obligation whatsoever; and the fact that the government may have formulated, furnished, or in any way supplied the said drawings, specifications, or other data, is not to be regarded by implication or otherwise as in any manner licensing the holder or any other person or corporation, or conveying any rights or permission to manufacture, use, or sell any patented invention that may in any way be related thereto.

This technical report has been reviewed and is approved for publication.

FOR THE DIRECTOR



R. F. Paulson
Project Engineer



Stanley E. Wagner, Chief
Electro-Optics Device Branch

Copies of this report should not be returned unless return is required by security considerations, contractual obligations, or notice on a specific document.

UNCLASSIFIED

SECURITY CLASSIFICATION OF THIS PAGE (When Data Entered)

REPORT DOCUMENTATION PAGE		READ INSTRUCTIONS BEFORE COMPLETING FORM
1. REPORT NUMBER AFAL-TR-75-4	2. GOVT ACCESSION NO.	3. RECIPIENT'S CATALOG NUMBER
4. TITLE (and Subtitle) 200 WATT COMPACT CO₂ LASER		5. TYPE OF REPORT & PERIOD COVERED Final Technical Report Nov 1973 to Dec 1974
		6. PERFORMING ORG. REPORT NUMBER
7. AUTHOR(s) Theodore S. Fahlen		8. CONTRACT OR GRANT NUMBER(s) F33615-74-C-1056
9. PERFORMING ORGANIZATION NAME AND ADDRESS GTE Sylvania, Inc. Electronic Systems Group Western Division, PO Box 188 Mountain View, California 94042		10. PROGRAM ELEMENT, PROJECT, TASK AREA & WORK UNIT NUMBERS 62204 F 2001 01 12
11. CONTROLLING OFFICE NAME AND ADDRESS AFAL/TEO Air Force Systems Command Wright-Patterson Air Force Base, Ohio 45433		12. REPORT DATE February 1975
		13. NUMBER OF PAGES 88
14. MONITORING AGENCY NAME & ADDRESS (if different from Controlling Office)		15. SECURITY CLASS. (of this report) UNCLASSIFIED
		15a. DECLASSIFICATION/DOWNGRADING SCHEDULE
16. DISTRIBUTION STATEMENT (of this Report) Distribution limited to U.S. Government agencies only; test and evaluation results reported; (February 1975). Other requests for this document must be referred to the Air Force Avionics Laboratory (AFAL/TEO), Wright-Patterson Air Force Base, Ohio 45433		
17. DISTRIBUTION STATEMENT (of the abstract entered in Block 20, if different from Report)		
18. SUPPLEMENTARY NOTES		
19. KEY WORDS (Continue on reverse side if necessary and identify by block number) CO₂ Laser compact laser		
20. ABSTRACT (Continue on reverse side if necessary and identify by block number) This final engineering report summarizes the work performed during a one-year program culminating in the developemtn of a compact, 200 watt, gas transport laser head, for (ultimately) airborne applications. The report describes the design, circulated, cooled gas through a large (400 cm³) glow discharge/optical cavity volume, over 200 watts of cw power, at a single wavelength (10.59μ), was generated by the laser head, with a total head efficiency of 6%. The laser head weighs less than 100 pounds, and has a maximum linear dimension of 24 inches and		

a volume of 3 feet³. The stable, (nine-pass "z" configuration) folded optical resonator cavity, vibrationally isolated from the main vacuum enclosure, produced a TEM₀₀ mode beam pattern with good beam amplitude and directional stability, at maximum power. A conceptual design of an entire airworthy laser system based on the head developed during the program is also presented in the report.

FOREWORD

This is the final engineering report on the "200 Watt Compact CO₂ Laser" prepared under Air Force Contract F33651-74-C-1056. This report was prepared by the Electronic Systems Group of GTE Sylvania, Inc., Mountain View, California, and describes work performed by the Electro-Optics Organization during the period 26 November 1973 to 26 December 1974. Dr. T. S. Fahlen was the principal investigator on this program with contributions from Mr. R. Kirk, Mr. R. Reynolds, and Mr. M. Conroy.

All work in this report was administered under the Air Force Avionics Laboratory, Air Force Systems Command, Wright-Patterson Air Force Base, Ohio. The Air Force Project Monitor was R. F. Paulson, (AFAL/TEO).

This report was submitted by the author December 30, 1974.

TABLE OF CONTENTS

<u>Section</u>	<u>Title</u>	<u>Page</u>
I	INTRODUCTION AND SUMMARY	1
II	LASER HEAD DESIGN	5
	2.1 Introduction	5
	2.2 General Operating Principles	5
	2.2.1 Electrode Configuration	7
	2.2.2 De-Excitation of Lower Level	8
	2.2.3 Flow Configuration	10
	2.2.4 Optical Cavity	10
	2.2.5 Summary	11
	2.3 Mechanical Design	12
	2.3.1 Center Section	18
	2.3.2 End Bells	20
	2.3.3 Blower	25
	2.3.4 Optical Cavity	25
	2.3.5 Electrode Structure	34
	2.4 Electronic Configuration	34
	2.4.1 General	34
	2.4.2 Discharge Configuration	37
	2.4.3 Discharge Configuration Experiments	37
	2.4.4 Final Electrode Configuration	39
	2.4.5 Final Discharge Characteristics	39
	2.5 Optical Design	40
	2.5.1 Resonant Cavity	40
	2.5.2 Collimator	44
	2.5.3 Power Monitor	47
III	LASER PERFORMANCE	51
	3.1 Output Power and Laser Head Efficiency	51
	3.2 Wavelength	52
	3.3 Transverse Mode Quality	55
	3.4 Amplitude Stability	59
	3.5 Beam Divergence and Angular Jitter	59

TABLE OF CONTENTS

<u>Section</u>	<u>Title</u>	<u>Page</u>
	3.6 Sealed Operating Life	62
	3.7 Environmental Tests	66
	3.7.1 General	66
	3.7.2 Temperature	67
	3.7.3 Ambient Pressure	68
	3.8 Summary and Conclusions	69
IV	CONCEPTUAL AIRWORTHY DESIGN	70
	4.1 Laser Head	70
	4.2 Power Supply	72
	4.3 Cooling System	73
	4.4 Gas Fill System	74
	4.5 Control/Monitor Panel	75
	4.6 Volume Reduction	75
	4.7 Summary	77
V	CONCLUSIONS AND RECOMMENDATIONS	79
VI	REFERENCES	83

LIST OF ILLUSTRATIONS

<u>Figure Number</u>	<u>Caption</u>	<u>Page</u>
1	200 Watt CO ₂ Laser	2
2	Diagram of Active Region	6
3	CO ₂ Energy Level Diagram	9
4	Vacuum Shell and Blower Assembly	13
5	Schematic of Cross Sectional Side View of Laser Head	14
6	Schematic of Top View of Laser Head	15
7	Schematic of End View of Cavity	16
8	Coolant Flow Path	17
9	Schematic of Center Section Weldment	19
10	Upstream End Bell	21
11	End Bell Support Plate	22
12	Downstream End Bell	23
13	Heat Exchanger	24
14	Variation of Laser Efficiency with Coolant Temperature	26
15	Blower Performance Curve - Atmospheric Conditions	27
16	One End of Cavity Assembly	29
17	Folding Mirror Holder	30
18	Folding Mirror Mount	31
19	Cavity Support Plate	32
20	Cavity Mirror Mounting Plate	33
21	Anode Structure	35
22	Electrical Schematic	36
23	Optical Cavity	41
24	Collimator Design Parameters	45
25	Collimator Lens Design	48
26	Schematic of Non-Output Mirror and Power Monitor	49
27	Power and Efficiency vs Input Current	53
28	Experimental Set Up for Transverse Mode Measurements	56
29	Beam Profile Without Aperture. Time Scale is 50 μ sec/div.	57
30	Beam Profile with Aperture. Top Trace: 10 msec/div., Bottom Trace 50 μ sec/div.	58

LIST OF ILLUSTRATIONS

<u>Figure Number</u>	<u>Caption</u>	<u>Page</u>
31	Experimental Arrangement for Measuring Amplitude Stability	60
32	Amplitude Stability. Upper Trace is Voltage Ripple on Power Supply; Lower Trace is Laser Beam Power	61
33	Beam Profile with Collimator. Time Scale: Upper Trace 20 msec/div, Lower Trace 200 μ sec/div.	63
34	Control/Monitor Panel	76

LIST OF TABLES

<u>Table Number</u>	<u>Caption</u>	<u>Page</u>
I	200W GTL Performance Characteristics	4
II	Power and Efficiency vs. Gas Mix at 4 Amps Discharge Current	54
III	Airworthy Laser Design	77

SECTION I

INTRODUCTION AND SUMMARY

The prime objective of this program was to develop a compact, lightweight carbon dioxide laser head capable of producing 200 watts of continuous power in the TEM₀₀ transverse mode. The laser was to operate on a single vibration-rotation transition (single P-line), have a high degree of beam amplitude and directional stability, meet specific beam size and divergence specifications, and operate at high electrical efficiency. (This program involved the development of the laser head only, and did not include gas handling equipment, power supplies, or control electronics.)

The projected systems application of the laser developed on this program requires an operational airborne, ruggedized design. Although the laser was not designed during this effort to full Mil-Spec requirements, the anticipated airborne environment was used as a design guide. To provide design information pertinent to a future flight model, the laser was to be briefly tested for its response to flight environmental conditions, to better identify areas for design improvement.

In view of the airborne application, this program included the conceptual design for a complete laser system that incorporates and is compatible with the laser head developed during this program. The design was to clearly outline the laser's growth potential for applications into a ruggedized, operational airborne system.

To meet the requirements placed on the laser, a design approach using recirculated transverse gas flow was taken. Figure 1 is a photograph of the laser head in operation with the output beam impinging on a fire brick. The laser head consists of a discharge/optical path region (the discharge is visible as a glow beneath the glass at the top of the device), an adjustable optical resonator cavity structure, two end bells (one of which contains a gas-to-liquid heat exchanger), and a vaneaxial blower to provide rapid closed cycle recirculation of the active gas medium through the discharge region and heat exchanger. The discharge, optic axis, and gas flow velocity are mutually orthogonal.

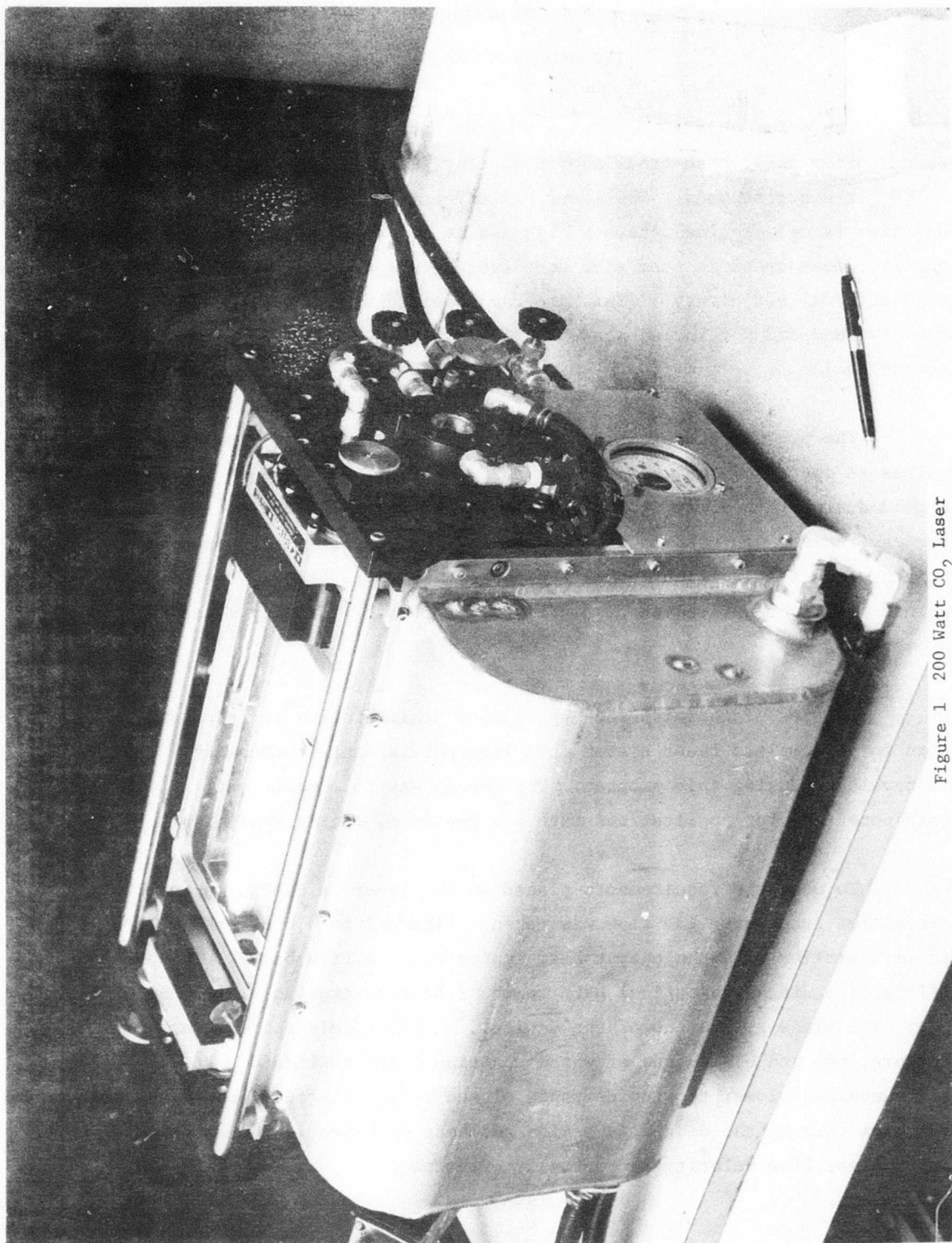


Figure 1 200 Watt CO₂ Laser

To save weight and volume, the system was designed to use tap water cooling so no external chiller is required. For the same reasons, the system was also designed to operate in a sealed off configuration, without a continuous replenishment of the laser gases. Therefore, during operation, no gas bottles, vacuum pump, and complementary valves and gauges are required.

A summary of the laser design specifications and actual performance specifications is given in Table I.

Over 200 watts of single wavelength, single mode power at 6% head efficiency are typical operating parameters. Amplitude stability was limited by the ripple inherent in the laboratory power supply. The degradation of output power with sealed off operating time and the laser head efficiency are two problems deserving more investigation.

Sections II and III of this report detail the design of the laser head and its performance characteristics, respectively. Section IV contains the conceptual design of an airworthy system based on the device fabricated and tested during this program. Section V contains recommendations for future development of this laser system.

Table I

200W GTL PERFORMANCE CHARACTERISTICS

<u>Parameter</u>	<u>Specification</u>	<u>Performance</u>
Output Power	200W	220W
Wavelength	Single P Transition	P(20) 10.59 μ
Mode	TEM ₀₀	TEM ₀₀
Amplitude Stability	5% P-P	6% P-P
Max. Far Field Divergence		
without collimator	2.5 mrad	1.8 mrad
with collimator	1.0 mrad	1.15 mrad
Max. Beam Diameter		
with collimator	16mm	20mm
Beam Directional Jitter		
without collimator	-	± 0.12 mrad
with collimator	± 0.2 mrad	$< \pm 0.2$
Power Degradation	5% in 4 hours	13% in 1 hour
Max. Volume	3 cu. ft.	3 cu. ft.
Max. Lin. Dimension	24 in.	24 in.
Head Efficiency	10%	6%
Head Weight	200 lbs.	97 lbs.

SECTION II

LASER HEAD DESIGN

2.1 INTRODUCTION

This section details the design of the 200W CO₂ laser head. Following a general discussion of the operating principles of the device are given detailed descriptions of the design of the mechanical structure (including the vacuum enclosure, vaneaxial gas recirculating blower, electrode structure, and optical cavity mounting structure), the design of the laser electrodes and ballast resistors, and the design of the optical elements (including laser mirrors, beam collimator, and beam power monitor).

2.2 GENERAL OPERATING PRINCIPLES

In general, the active medium of a "carbon dioxide" laser consists of a mixture of CO₂, N₂, and He gases at a total pressure of several 10's of torr. Under proper conditions, laser radiation at 10.6μ is generated from the CO₂ molecule upon its excitation, directly or indirectly, in a glow discharge. To achieve high cw power and high efficiency, the following criteria, among others, must be met.

- 1) To obtain efficient upper laser level excitation, a uniform discharge having the proper electronic energy distribution must be maintained throughout the active volume of gas.
- 2) The population density in the lower laser level, waste heat, must be rapidly removed to achieve efficient, powerful laser action.
- 3) To obtain high power in a small volume, the discharge must be maintained at as high a gas pressure as possible.
- 4) The optical beam must be efficiently coupled to the active discharge volume.

The following paragraphs explain how these criteria are met in the laser designed on this program. To orient the reader to the relationships among gas flow velocity, optical cavity configuration, and electrode configuration as fabricated during this program, a schematic of the active laser region is shown in Figure 2.

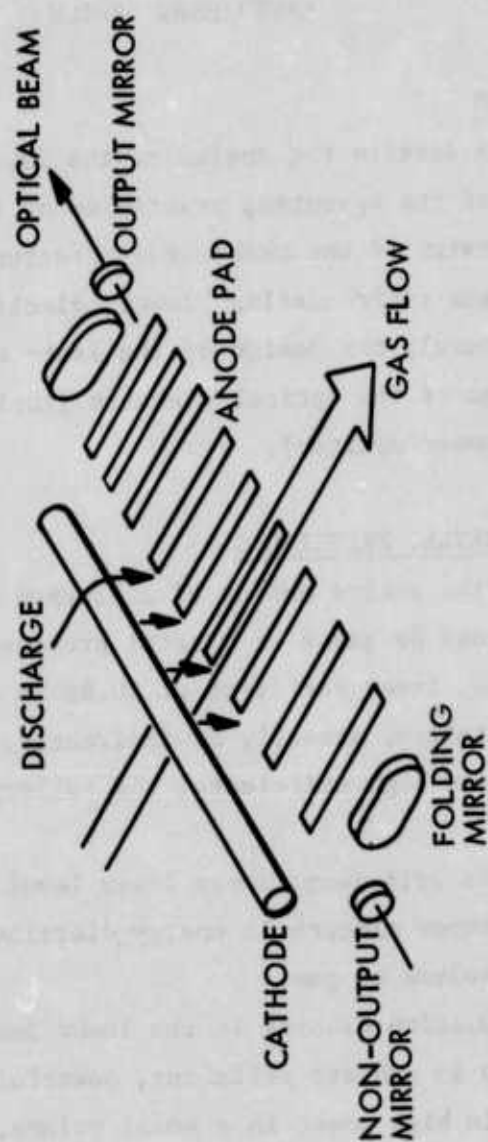


FIGURE 2 DIAGRAM OF ACTIVE REGION

2.2.1 Electrode Configuration

In a conventional longitudinal discharge tube, the excitation field is applied lengthwise down a long tube parallel to the optic axis of the laser. For reasons discussed below, the diameter of the tube can only be a few centimeters so that to obtain a large volume for high power, a long tube is required. Such a tube is not only cumbersome but requires the use of high voltages. A more viable alternative is to use a transverse discharge, i.e., one with ratio of electrode length to discharge length greater than unit. Usually, the transverse discharge is perpendicular to the optic axis. Such a discharge can provide the required E/p at much lower voltages (and higher currents) over large discharge volumes. As will be discussed below, to provide sufficient gas cooling, the gas is moved at high velocity through the discharge region. A transverse discharge can be maintained either parallel or perpendicular to the gas flow. If parallel to the gas flow, the pressure drop due to the electrode structure in the flow stream will reduce the gas velocity. Therefore, to obtain low voltage (high current) operation (an important consideration in airborne systems), to allow the electrodes to be located out of the gas stream, and to ease fabrication difficulties and costs, the chosen design utilizes a discharge transverse to both the gas flow velocity and optic axis of the laser.

One of the prime problems is maintaining a uniform, stable discharge over a large volume of gas. The problem becomes more difficult as the gas pressure is increased. To provide arc-free operation a single, cylindrical cathode running parallel to the optical beam is located above and upstream of several anode pads which form the floor of the discharge channel. Each anode pad is individually ballasted to limit the current through it.

The discharge and optical beam volume are designed to extend downstream the length of the anode pads. No magnetic field is required to confine the discharge in a narrow active region; discharge and excited gas blown downstream is still within the optical resonant cavity and is therefore useful.

2.2.2 De-Excitation of Lower Level

The decay rate of the upper level to the ground state is much slower than is either the transition rate from the 100 to the 010 level or from the 020 level to the 010 level, so that a population inversion between the upper and lower laser levels can occur. (Figure 3 shows an energy level diagram for CO_2 .) However, the decay of the 010 level is fairly slow. Consequently, this level is a bottleneck in the decay chain, increasing the 100 level population and reducing the laser level inversion. To achieve efficient, powerful laser action, it is important then to provide a means for eliminating this bottleneck.

One way of accomplishing this is to add He gas to the $\text{CO}_2\text{-N}_2$ mix to collisionally cool the 010 energy level. The addition of He may also aid laser action by controlling the energy of the discharge electrons.

Another method of lowering the population of the 010 level is to physically remove the CO_2 molecules after they have produced their laser photons. Such a technique is termed convection cooling the gas. In a diffusion cooled laser, waste energy (in the form of CO_2 gas excited to the 010 level) is removed as hot gas diffuses to a cool wall. The characteristic diffusion cooling time, τ_o , is therefore⁽¹⁾

$$\tau_o \propto \frac{D^2}{Lv_t}$$

where D is the characteristic dimension of the discharge, L is the gas molecule mean-free path, and v_t is the gas molecule thermal velocity. In a convectively cooled system with a gas flow velocity of v , the characteristic cooling time, τ_f is

$$\tau_f = D/v.$$

The ratio of achievable laser power in the two cases P_o/P_f is proportional to τ_f/τ_o or Lv_t/Dv . At 25 t and 400°K , $Lv_t \approx 200 \text{ cm}^2\text{sec}^{-1}$ for He (best case). Therefore, even for nominal gas velocities, $P_f \gg P_o$ for the same volume and gas

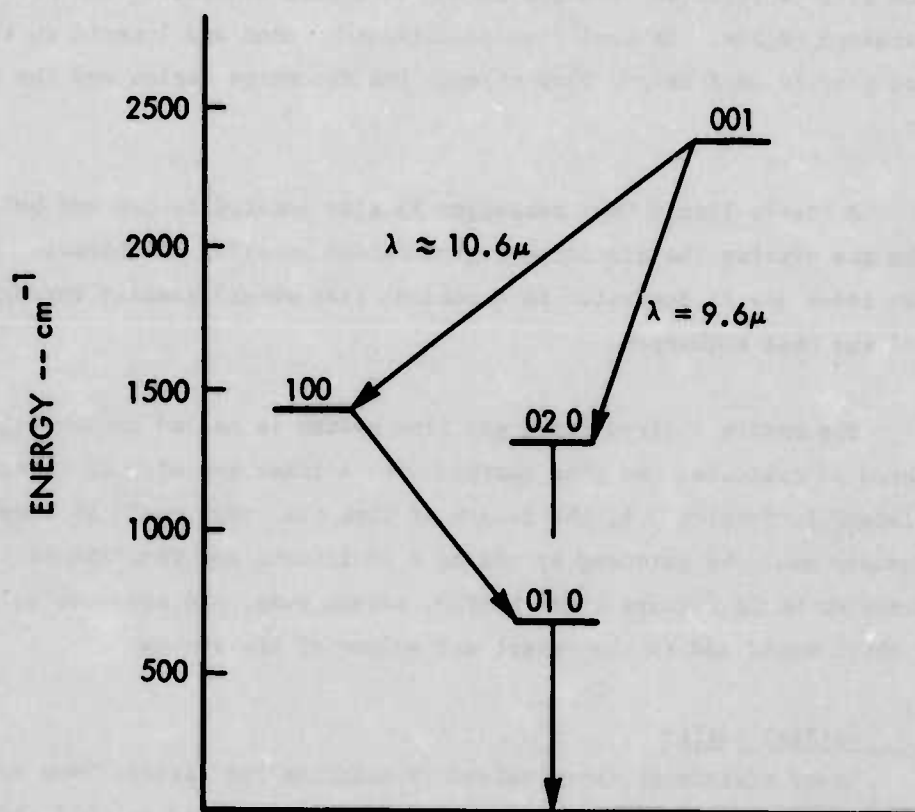


FIGURE 3 CO₂ ENERGY LEVEL DIAGRAM

density. The design chosen, then, is to provide a rapid gas flow across a narrow active region to provide a greater power output capability by physically removing the molecules in the lower laser level.

2.2.3 Flow Configuration

To satisfy the requirements of the lower laser level de-excitation discussed in Section 2.2.4, the gas flow velocity is directed perpendicularly to the optic axis of the laser. The flow velocity is as high as possible, as it has been shown ^(1,2) that laser output power is proportional to the gas flow velocity. A vaneaxial blower (discussed in detail in Section 2.3.3) contained within the laser vacuum shell provides a flow velocity of 40-50 m/sec. Two "end bell" structures form the vacuum enclosure connecting the blower to the discharge region. Several flow conditioning vanes are located in these end bells to provide uniform gas flow through the discharge region and the heat exchanger.

A gas-to-liquid heat exchanger is also located in one end bell to cool the gas exiting the discharge region before entering the blower. Heat from the laser gas is deposited in a coolant (tap water) passing through the tubes of the heat exchanger.

The entire recirculating gas flow system is sealed vacuum tight. Once the system is evacuated and then charged with a laser gas mix, it is sealed off. As explained in Section 3.6, the length of time the laser could be operated continuously could be extended by adding a continuous gas replenishment system. Such a system would require a gas bottle, vacuum pump, and assorted valves and gauges which would add to the weight and volume of the system.

2.2.4 Optical Cavity

Laser efficiency is optimized by matching the optical beam volume to the active discharge volume. Two flat mirrors are employed to fold the beam so that it makes nine transits of the discharge region in traveling from one cavity mirror to the other. This also permits a more advantageous use of the volume (3 cubic feet) specified for the laser head.

Two general cavity configurations can be considered: unstable, and stable. The unstable resonator has the advantage of greater power extraction from a high-gain laser medium, which CO_2 is, but has the disadvantage of producing an output beam of greater divergence and less far field axial intensity, when compared to a stable resonator. Because the proposed application of the

laser requires a good far field pattern, with high on-axis power density, a stable resonator cavity was chosen.

The stable resonator cavity consists of a flat output mirror, and a long radius of curvature, spherical non-output mirror. The individually adjustable, water cooled mirrors are mounted in a rigid structure vibrationally isolated from the main laser structure to reduce amplitude and directional beam instabilities.

Off-axis and transverse mode suppressing apertures are used to prevent parasitic oscillations from occurring. A thermopile in thermal contact with the rear, non-output laser mirror can be used to monitor the laser output beam power by monitoring the small amount of intracavity power absorbed by the rear mirror. The design of the power monitor is discussed in Section 2.5.3.

Mounted externally to the laser output mirror is a two element beam collimator designed to collimate the output beam to better than 1 mrad.

2.2.5 Summary

The 200W gas transport laser (GTL) developed on this program utilizes a transverse glow discharge to directly and indirectly electrically excite the upper laser level of CO_2 throughout a large volume of gas, a vaneaxial blower to provide a high laser gas flow velocity to convectively remove the waste discharge heat and lower laser level population from the active laser region to an enclosed gas-to-liquid heat exchanger, and a folded, stable optical resonator cavity. During operation, the laser is sealed off. The technological base for the development of this laser was derived from the development of the GTE Sylvania Model 971 Gas Transport Laser which produces 1000W of cw TEM_{00} mode power at 10.6μ . The 200W GTL developed here is a scaled down version of the 1000W device.

The following paragraphs detail the mechanical, electrical, and optical design of the laser developed during this program.

2.3 MECHANICAL DESIGN

The laser head consists of the following primary components:

- 1) The center section which contains the laser electrodes and active laser volume,
- 2) An upstream end bell which joins the output end of the fan housing to the input end of the center section and contains gas flow conditioning vanes,
- 3) A downstream end bell which joins the input end of the fan housing to the output end of the centersection and contains the gas-to-liquid heat exchanger,
- 4) A fan housing which contains the vaneaxial fan, and
- 5) The resonant cavity optical mount structure which encloses two opposite sides of the center section and holds the laser optics.

An exploded isometric schematic of the laser head vacuum shell (without the optics) is shown in Figure 4. A more detailed side view of the head (without the optics) is depicted in Figure 5. A top view of the center section and optical cavity mount structure is shown schematically in Figure 6, and an end view of the resonator cavity is depicted in Figure 7.

To ensure vacuum integrity, all vacuum shell joints between removable sections are "O"-ring sealed and all permanent joints are sealed with epoxy. To save weight, the vacuum shell is made entirely of aluminum with the exception of a glass discharge viewing port forming the top of the center section. The two top invar rods are attached to flanges on the end bell support plates by means of rubber mounting brackets to damp out vibrations.

All mirrors and both anode and cathode as well as the heat exchanger are water cooled. The total coolant flow rate is approximately 2 gpm. The coolant path is shown schematically in Figure 8.

When assembled, the laser head has a measured rate of pressure rise of 1.6 mtorr per minute corresponding to a leak rate of less than 7×10^{-4} atm cm^3/sec .

The envelope of the laser head, excluding the collimator, is 24 inches long, 16 inches high, and 13.5 inches wide or 3 cubic feet. The head weighs 97 pounds. The gas volume is $2.2 \times 10^4 \text{ cm}^3$ (0.78 ft.³).

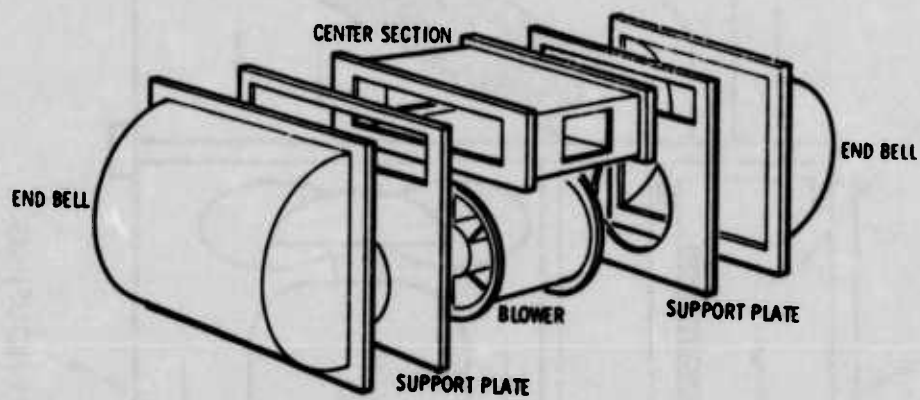


Figure 4 Vacuum Shell and Blower Assembly

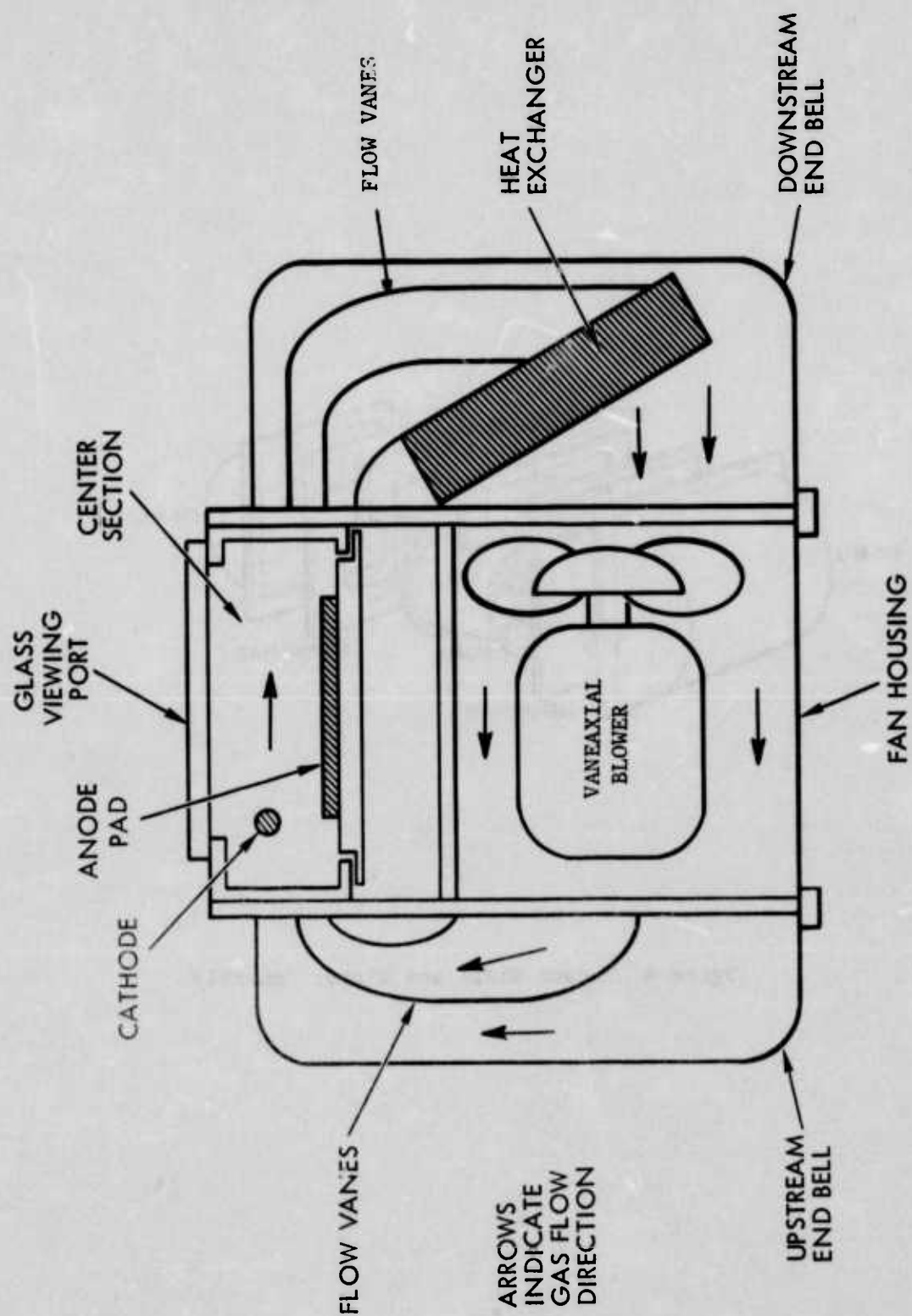


Figure 5 Schematic of Cross Sectional Side View of Laser Head

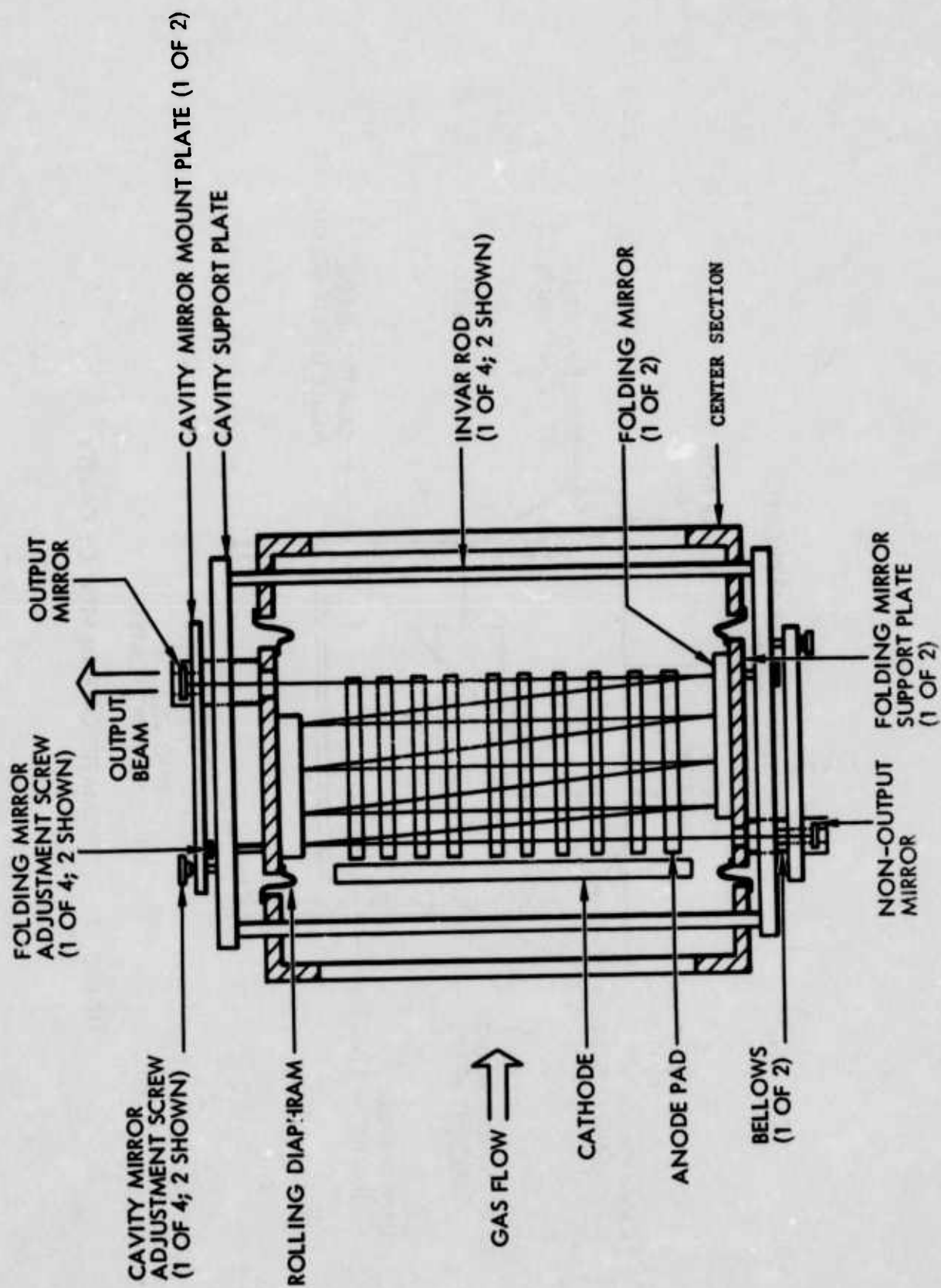


Figure 6 Schematic of Top View of Laser Head

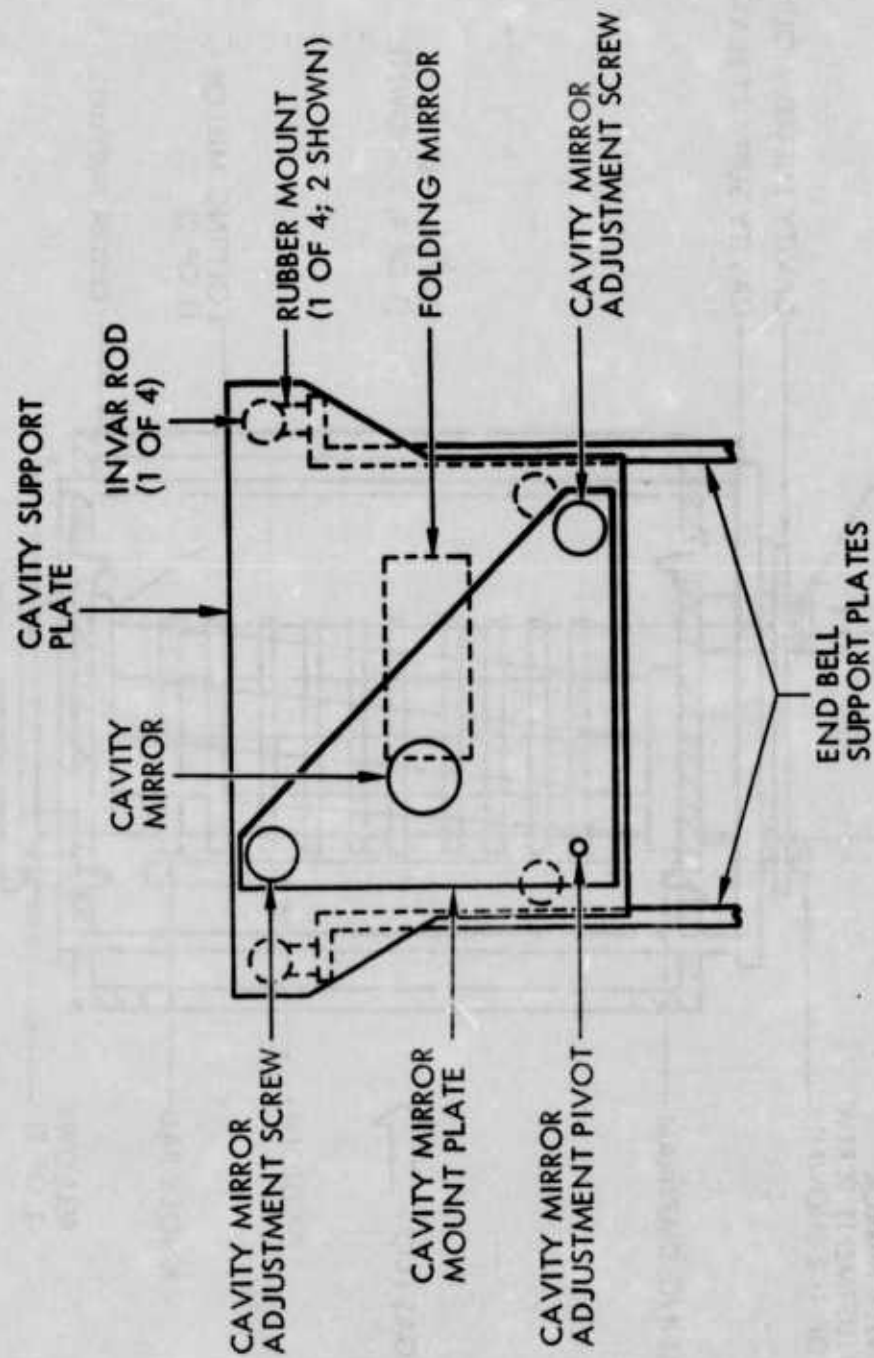


FIGURE 7 SCHEMATIC OF END VIEW OF CAVITY

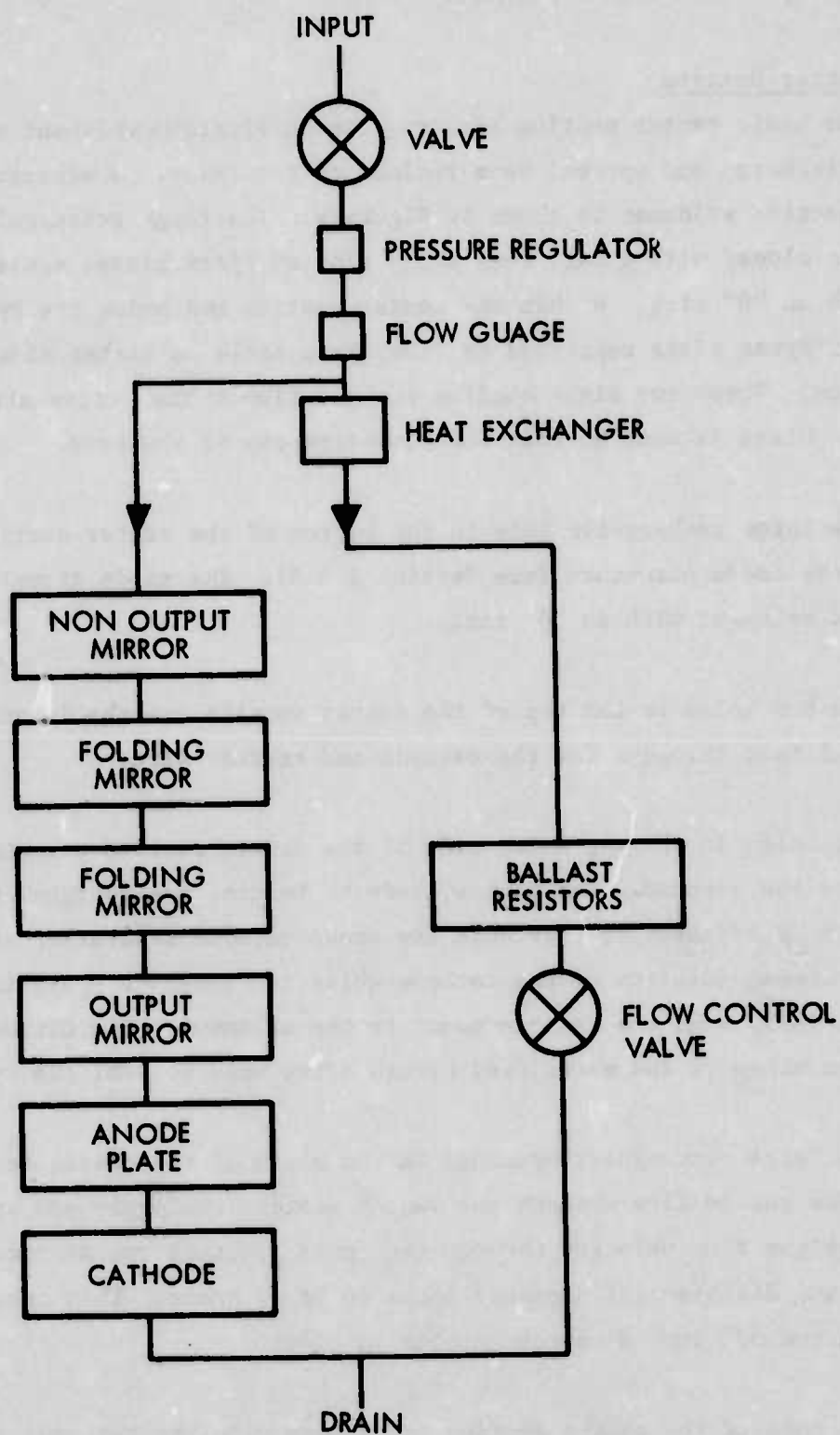


FIGURE 8 COOLANT FLOW PATH

The following paragraphs detail the mechanical design of each of the five primary laser head components.

2.3.1 Center Section

The basic center section structure is an aluminum weldment enclosing the active discharge and optical beam regions of the laser. A schematic of the center section weldment is shown in Figure 9. The large rectangular hole in the top is closed with a half inch thick slab of Pyrex glass, sealed to the weldment with an "O" ring. Within the center section and below the Pyrex slab are two other Pyrex slabs supported by fiberglass rails on either side of the center section. These two slabs confine the gas flow to the active discharge area. Glass is used so that the discharge can be observed.

The large rectangular hole in the bottom of the center section is taken up by the anode structure (see Section 2.3.5). The anode structure is sealed to the weldment with an "O" ring.

The two holes in the top of the center section are the locations of the electrical feed throughs for the cathode and starter wire.

Two holes in the gas inlet side of the center section are where the cathode mounts are located. The mounts, made of Delrin, are designed to allow the cathode to be adjusted to vary both the anode-cathode separation and the upstream-downstream location of the cathode while the laser is operating. Both "O" rings and epoxy seal the cathode mount to the weldment. The cathode mount is also the location of the water feedthrough lines used to cool the cathode.

The large rectangular openings in the sides of the center section allow the laser gas to flow through the center section uniformly and at high velocity. The gas flow velocity through the center section was measured with a Pitot tube and differential pressure gauge to be 42 m/sec. This measurement was made with the 5/8 inch diameter cathode in place.

The ends of the center section are sealed with the resonant cavity optics. The optics are sealed to the weldment by clamping one edge of a circular rolling rubber diaphragm to the optics and one edge to the weldment.

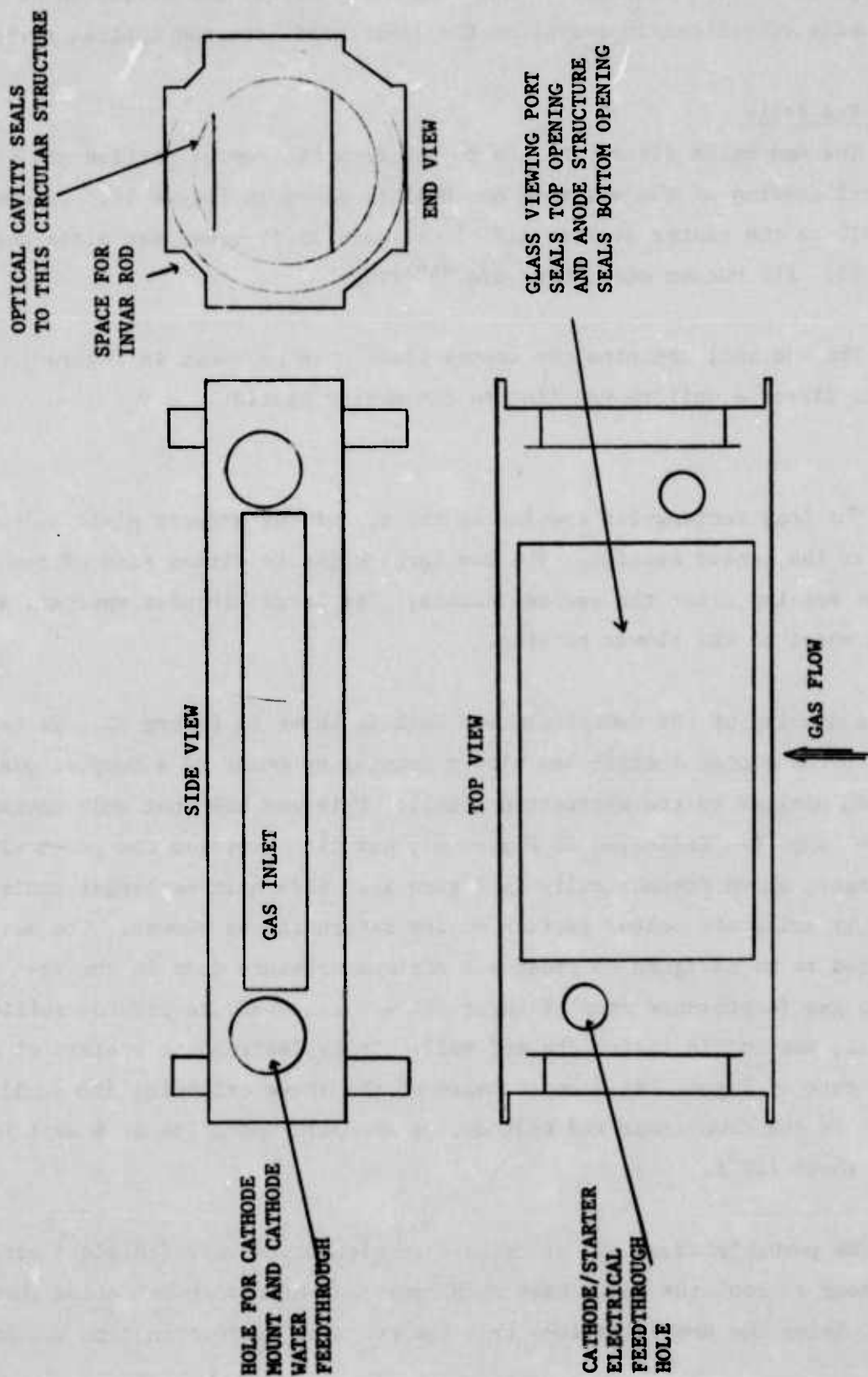


Figure 9 Schematic of Center Section Weldment

Such a diaphragm forms a flexible vacuum seal which allows the mirror to be adjusted while vibrationally isolating the laser head from the optical cavity.

2.3.2 End Bells

The end bells direct the gas to and from the center section and blower. A mechanical drawing of the upstream end bell is shown in Figure 10. Joining the end bell to the center section and blower housing is a support plate shown in Figure 11. All vacuum seals here are "O"-rings.

The end bell contains two copper flow vanes as shown in Figure 5. These vanes direct a uniform gas flow to the center section.

The long rectangular opening at the top of the support plate allows gas to enter the center section. The two large holes to either side of the rectangular opening clear the cathode mounts. The large circular aperture at the bottom mates to the blower housing.

A drawing of the downstream end bell is shown in Figure 12. It is connected to the center section and blower housing by means of a support plate in a fashion similar to the upstream end bell. This end bell not only contains copper flow vanes (as indicated in Figure 5), but also contains the gas-to-liquid heat exchanger, shown schematically in Figure 13. This heat exchanger cools the gas as it exits the center section on its return to the blower. The heat exchanger had to be designed to produce a minimum pressure drop in the recirculating gas (a pressure drop of about 10% was achieved), to provide sufficient heat removal, and to fit inside the end bell. It is designed to operate at a water flow rate of 1 gpm. As a consequence of the above criteria, the equilibrium temperature of the downstream end bell during standard operation at 4 amps input current is about 120°F.

The possible advantage of using a refrigeration unit (chiller) outside the laser head to cool the laser heat exchanger coolant was investigated theoretically. Using the approximations that the power is proportional to the gain which

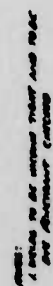
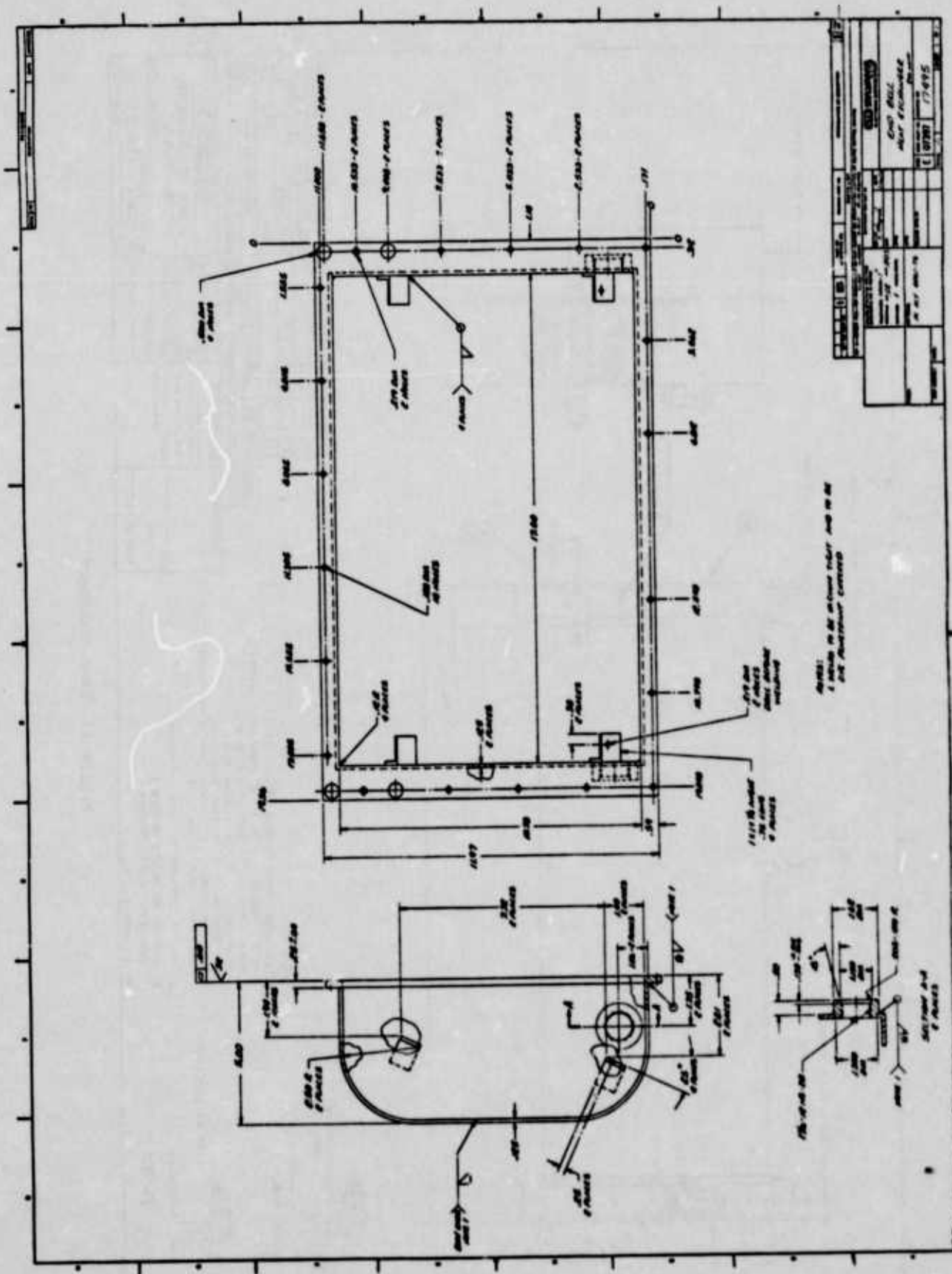


Figure 10 Upstream End Bell

1	2	3	4	5	6	7	8	9	10	11	12	13	14	15	16	17	18	19	20	21	22	23	24	25	26	27	28	29	30	31	32	33	34	35	36	37	38	39	40	41	42	43	44	45	46	47	48	49	50	51	52	53	54	55	56	57	58	59	60	61	62	63	64	65	66	67	68	69	70	71	72	73	74	75	76	77	78	79	80	81	82	83	84	85	86	87	88	89	90	91	92	93	94	95	96	97	98	99	100
---	---	---	---	---	---	---	---	---	----	----	----	----	----	----	----	----	----	----	----	----	----	----	----	----	----	----	----	----	----	----	----	----	----	----	----	----	----	----	----	----	----	----	----	----	----	----	----	----	----	----	----	----	----	----	----	----	----	----	----	----	----	----	----	----	----	----	----	----	----	----	----	----	----	----	----	----	----	----	----	----	----	----	----	----	----	----	----	----	----	----	----	----	----	----	----	----	----	----	-----



varies as the inverse $3/2$ power of the gas temperature, we obtain the curve depicted in Figure 14. Here, the change in laser head efficiency is plotted as a function of coolant temperature. It is seen that even at a coolant temperature of -20°C , the practical limit of refrigeration units, the increase in laser efficiency is only 1.3%, from 6% to 7.3%. The decrease in overall laser efficiency due to the added power consumed by a refrigeration unit would be much greater than the slight increase in laser head efficiency. The use of a chiller is not, therefore, a practical way to increase overall laser efficiency.

2.3.3 Blower

The blower housing is a 7 inch diameter by 7.5 inch long cylinder with parallel end flanges. These flanges are sealed to the two end bell support plates with "O"-rings. The blower housing contains the vaneaxial blower and flow conditioning vanes. The blower operates with 215 watts of 208V, 400 Hz power. The blower performance characteristics are shown in Figure 15. The blower was chosen to be compact, lightweight, capable of being cooled by the gas flow stream, and capable of providing a sufficient mass flow rate.

The blower was obtained from Dynamic Air Engineering (modified part No. M6921H-1A with motor No. M3018313C). Modifications pertain to the flanges for flatness and parallelness ("O"-ring sealing) and vacuum properties.

2.3.4 Optical Cavity

The resonant cavity consists of a partially transmitting output mirror, a totally reflecting non-output mirror, and two large flat folding mirrors. The optical beam makes nine passes through the active discharge area as indicated in Figure 6.

To provide stable operation, the optical cavity was designed as an integral structure to be mounted to, but vibrationally isolated from the main laser structure. A rough schematic of the optical cavity structure is shown in Figure 6 and Figure 7. Four invar rods 20.375 inches long by 0.625 diameter rigidly join the two cavity support plates. The two rods located above the

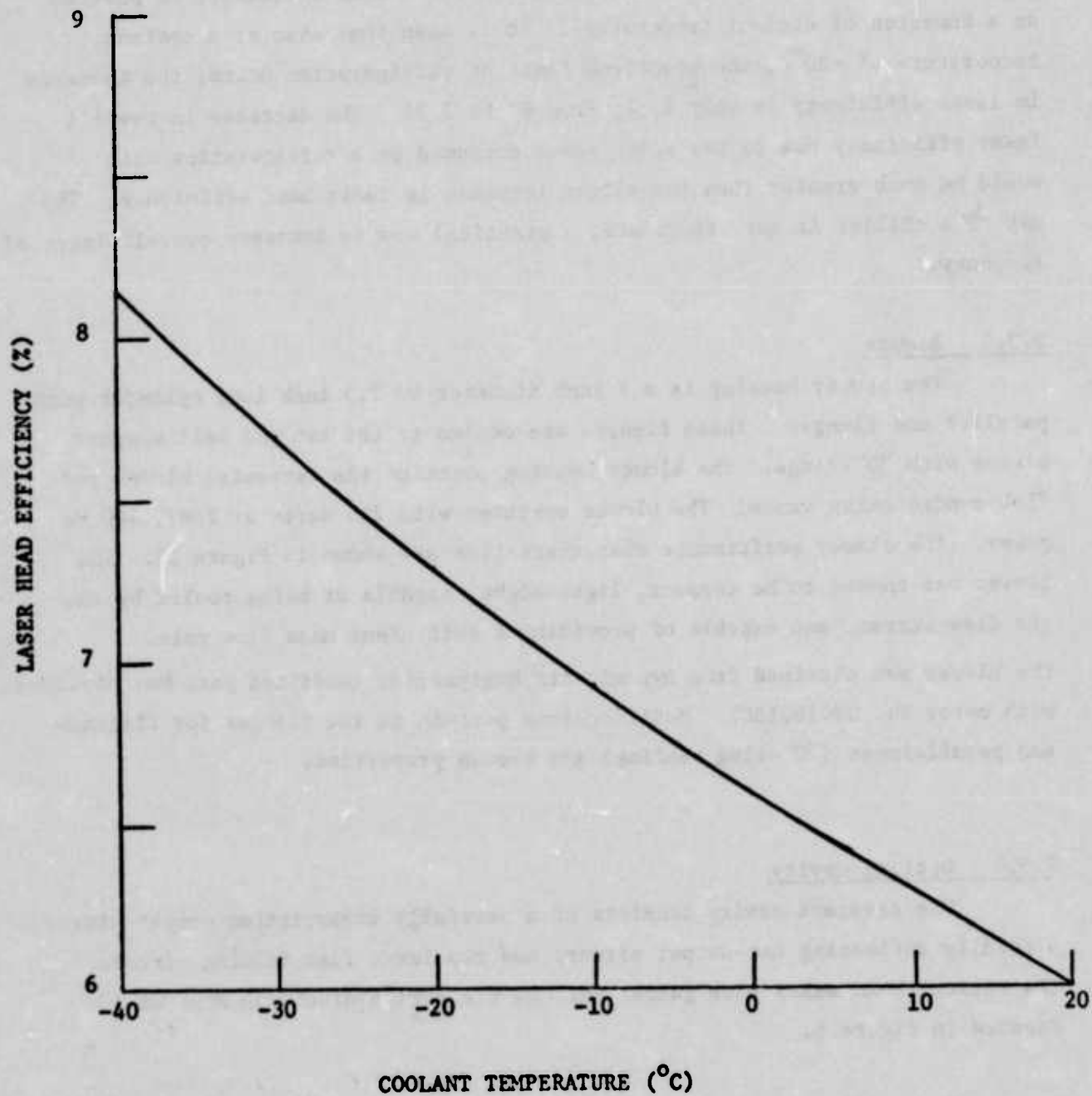


Figure 14 Variation of Laser Efficiency with Coolant Temperature

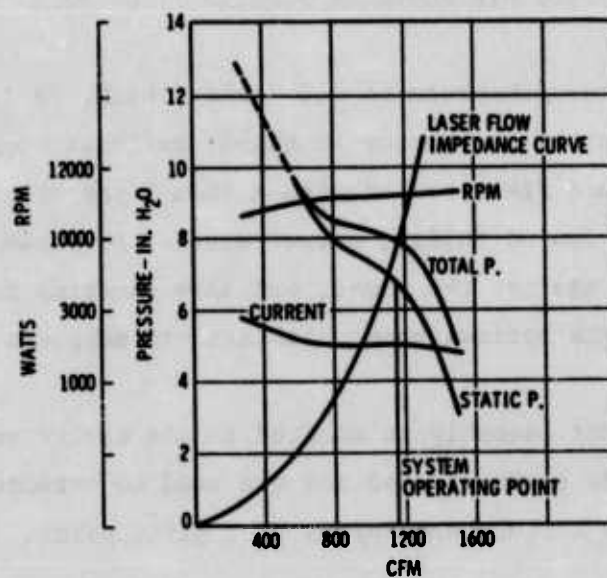


Figure 15 Blower Performance Curve - Atmospheric Conditions

centersection are connected to the end bell support plates by four rubber isolators. The two rods passing between the center section and blower housing are not attached to the vacuum shell.

The cavity mirror mounting plates are attached to the two cavity support plates. Figure 16 is a diagram of one end of the cavity assembly. Drawings of the folding mirror holder, folding mirror mount, cavity support plate, and cavity mirror mounting plate are shown in Figures 17 to 20.

The folding mirror substrate is 0.5 inches thick, by 1.5 inches wide by 3 inches long. The front of the mirror is highly reflective and flat. The rear surface is ground flat, coated with a thin layer of oil, and pressed against the flat, water cooled folding mirror mount. A retaining plate not only presses the mirror against the mount, but also contains four apertures tilted with respect to the optical beam which act to suppress off axis modes.

The folding mirror assembly is mounted to the cavity support plate with three invar rods; two are spring loaded and are used to orthogonally adjust the angular alignment of the mirror, one serves as a pivot point.

The output mirror is sealed in a water cooled holder with a pressed indium seal. The holder is bolted to the cavity mirror mounting plate which in turn is attached to the cavity support plate with two orthogonal adjustment screws and one invar flexure which acts as a pivot point. The adjustment screws were originally to be differential micrometers, but it was found in practice that single 40 pitch screws were quite sufficient.

A removable transverse mode controlling aperture is located directly on the vacuum side of the non-output mirror. A metal bellows serves as a vacuum enclosure between the folding mirror mount and the cavity mirror mount. The reference plane for all mirror adjustments is the plane containing the ends of the four invar support rods.

Details of the mirrors themselves are discussed in Section 2.5.1.

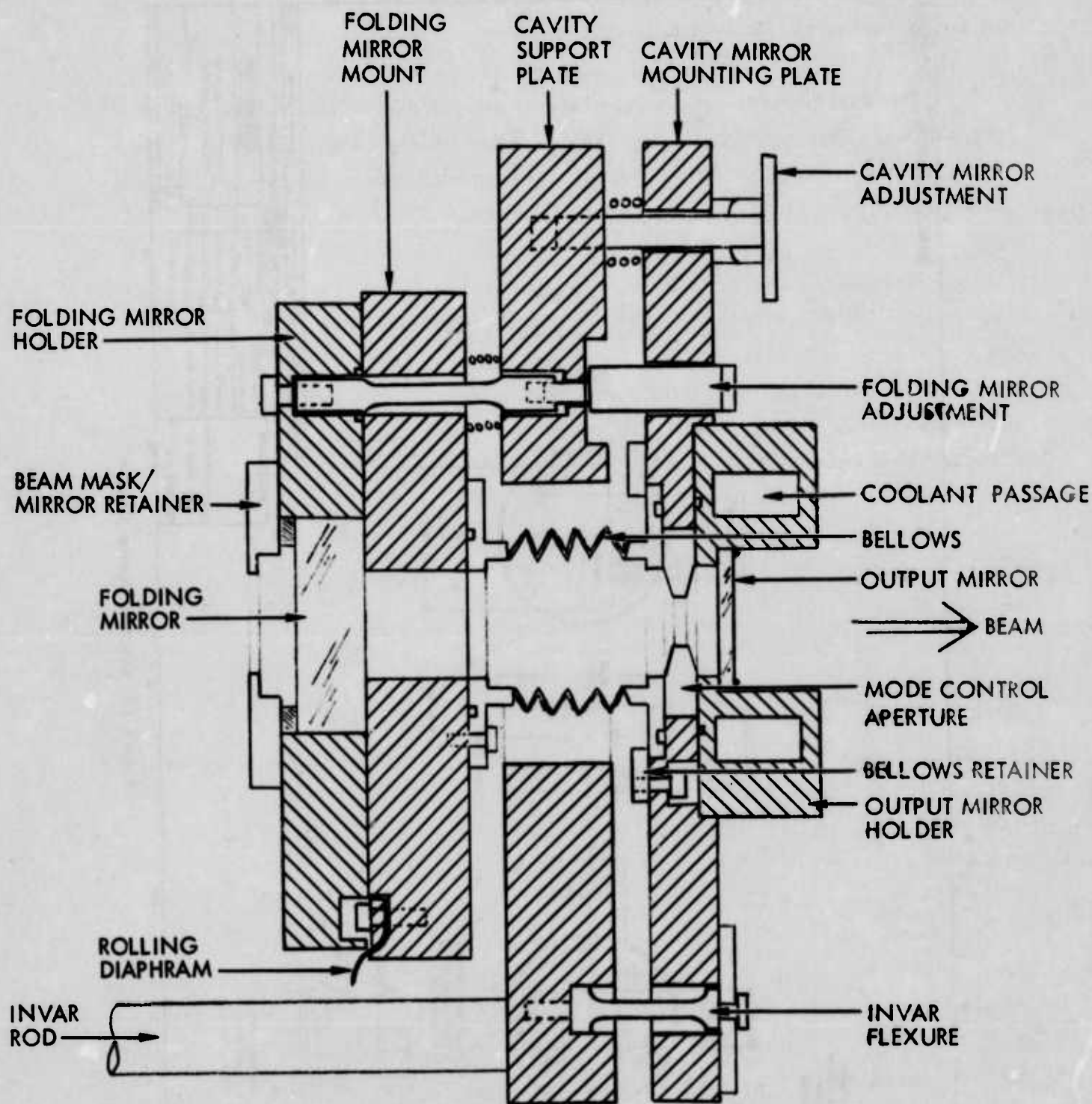


FIGURE 16 ONE END OF CAVITY ASSEMBLY

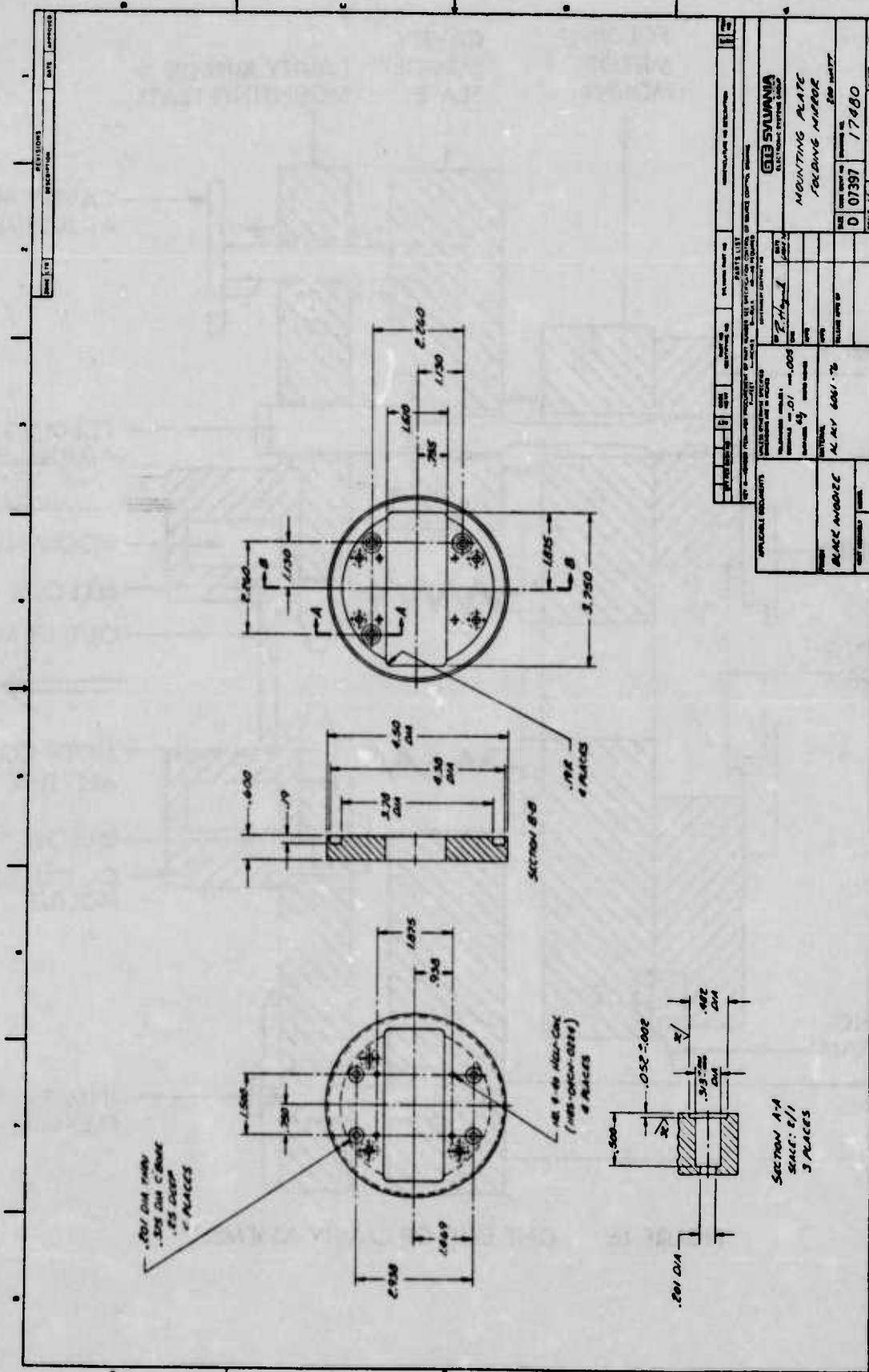


Figure 17 Folding Mirror Holder

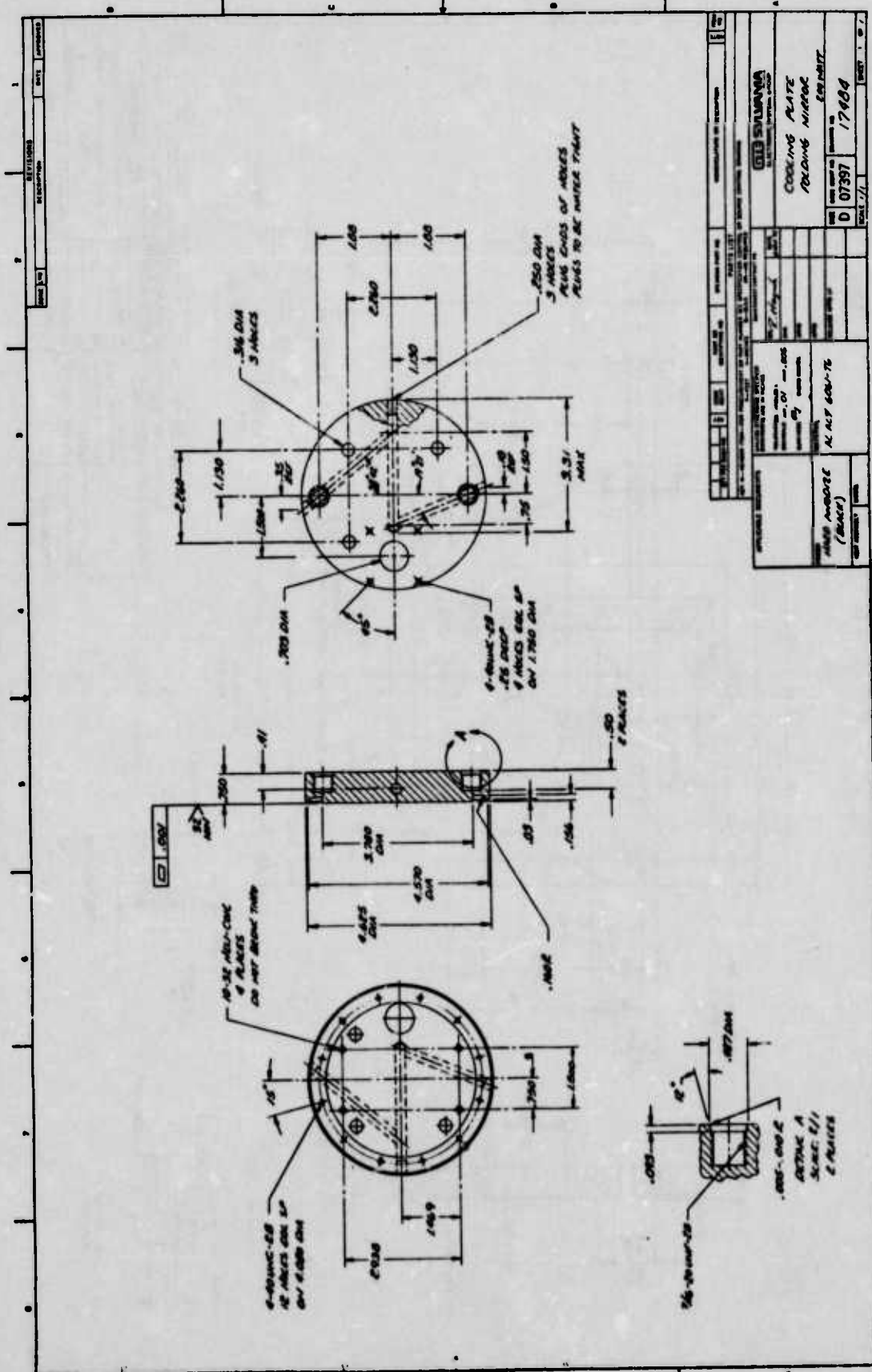


Figure 18 Folding Mirror Mount

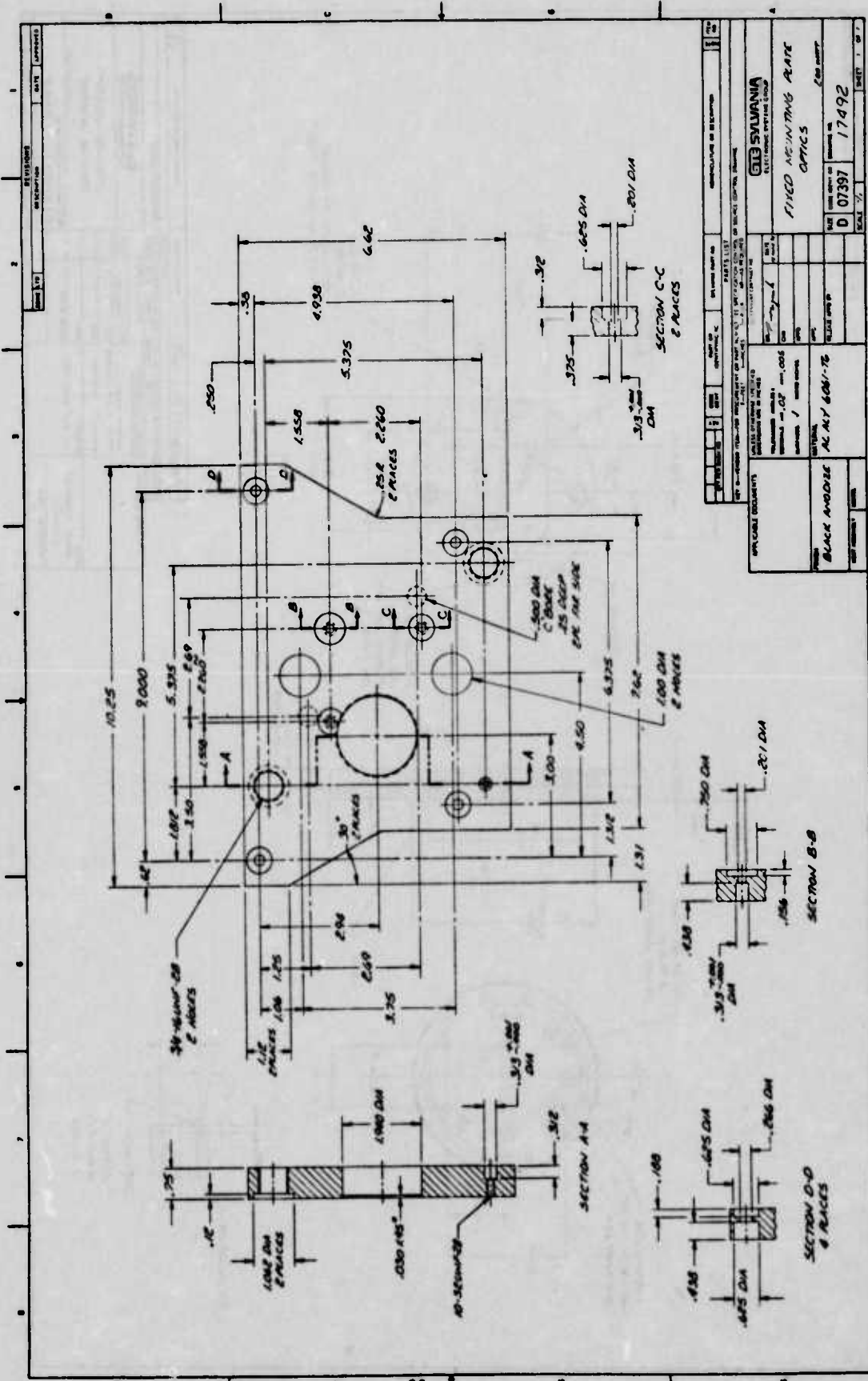
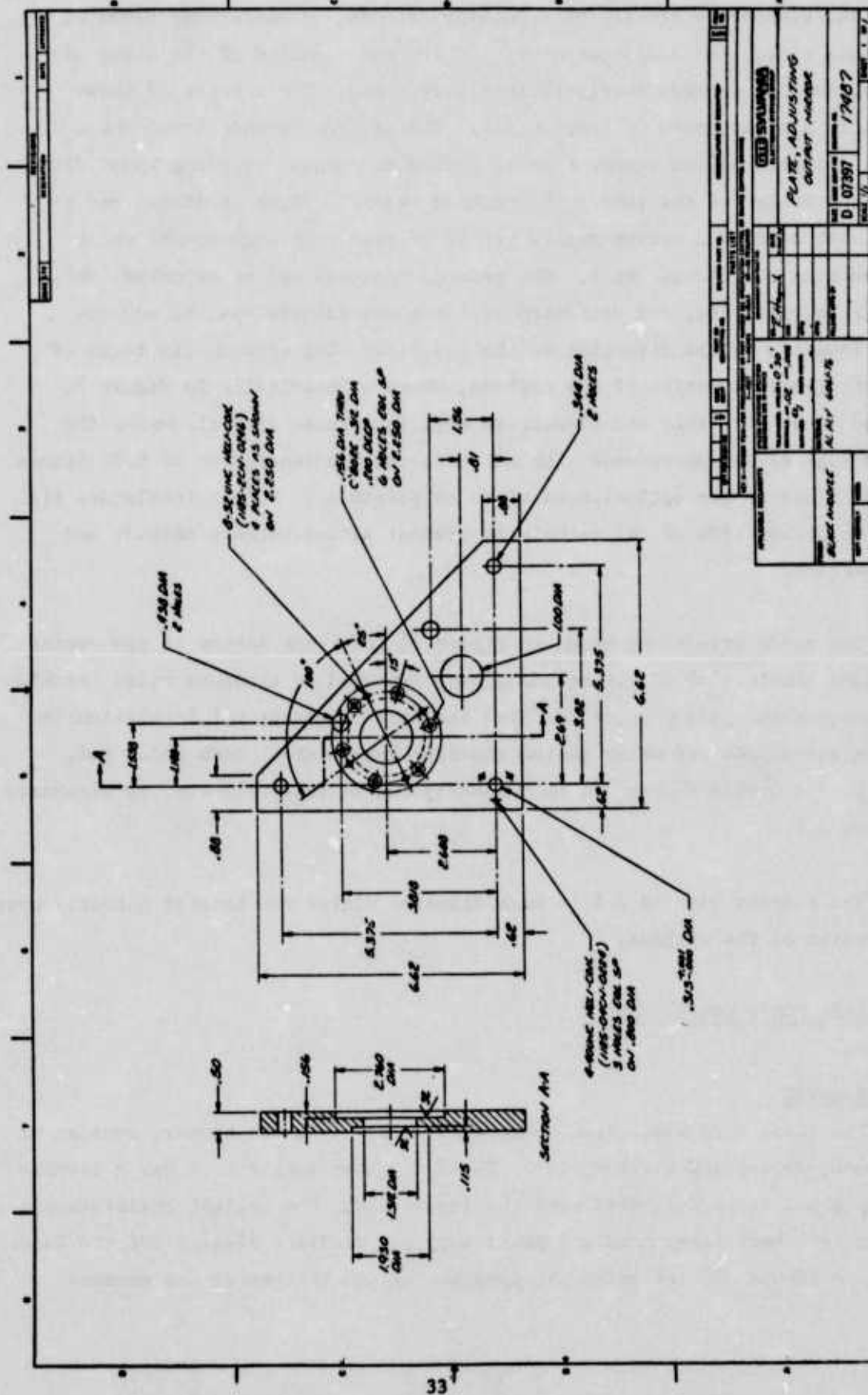


Figure 19 Cavity Support Plate



2.3.5 Electrode Structure

The electrodes consist of a tubular cathode, 18 anode pads cemented in an anode plate, and a starter wire. During maximization of the laser efficiency, several cathode configurations were tried. The results of these experiments are discussed in Section 2.4. The optimum cathode found was a 5/8 inch diameter hollow copper tube 13 inches in length. Cooling water flows through the center of the tube. The cathode uses "O"-rings at either end to provide both water and vacuum seals. It is mounted in Delrin mounts which extend outside the vacuum shell. The cathode position can be adjusted, while the laser is operating, for variation of the anode-cathode spacing and the cathode location in the direction of the gas flow. The optimum (in terms of laser efficiency) location of the cathode, shown schematically in Figure 5, was found to be such that its downstream edge is located directly above the upstream edge of the anode pads with an anode-cathode separation of 0.70 inches (i.e., as close to the optical beam width as possible). Delrin insulators are located on either side of the cathode to prevent arcing between cathode and center section.

The anode structure, shown in Figure 21 forms the bottom of the center section and consists of 18 copper anode pads cemented to aluminum oxide ceramic pads. The ceramic pads provide the high temperature electrical insulation between the anode pads and water cooled aluminum base plate. Each anode pad, 3.173 x 0.47 x 0.0625 inches, is individually resistively ballasted as discussed in Section 2.4.

The starter wire is a 1/16 inch diameter nickel rod located directly upstream of the center of the cathode.

2.4 ELECTRONIC CONFIGURATION

2.4.1 General

The laser head electrical components, other than the blower, consist of the cathode, anode, and starter wire. The d.c. power supply used was a laboratory supply not to be delivered with the laser head. The ballast resistors are separated from both laser head and power supply. A wiring diagram for the laser is shown in Figure 22, including the location of the volt-meter and ammeter.

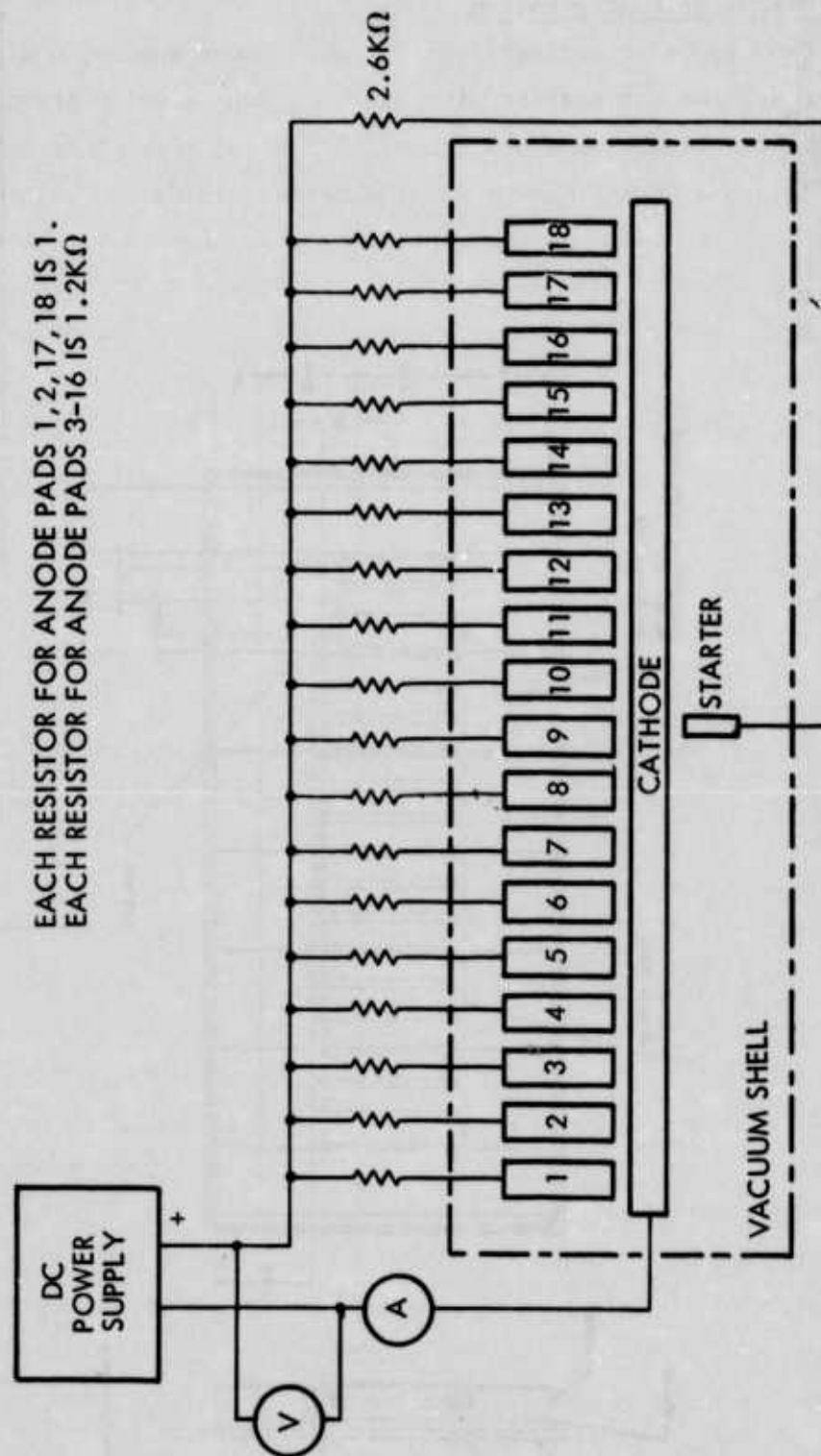


FIGURE 22 ELECTRICAL SCHEMATIC

2.4.2 Discharge Configuration

Upon applying voltage from the d.c. power supply, a discharge is initiated between the starter wire and the cathode which provides uniform ionization of the gas near the center of the cathode. Increasing the applied voltage causes a normal glow discharge between anode and cathode near the center of the cathode. As the input current is raised to the 4 amp operating range the discharge spreads out toward either end of the cathode and provides a uniform discharge between anode and cathode. With the standard gas mix of 25 tHe, 10 tN₂, and 2.5 tCO₂, the total voltage applied to the discharge, starter wire, and ballast resistors is 1150V at 4 amps. Here the discharge extends visually over about 2/3 of the anode pad length parallel to the gas flow.

2.4.3 Discharge Configuration Experiments

There is some indication that there is a lack of optical gain in the discharge region above the downstream portion of the anode pads (see Section 2.5.1). Because one possible cause of this lack of gain is that the downstream gas is not sufficiently electrically excited, several cathode-anode configurations were tried in an effort to extend the visible discharge farther downstream along the anode pads.

The first cathode used was a streamlined cathode having a cross section resembling an airfoil. With this cathode, the gas flow velocity was measured to be about 25% faster than that obtained with the 5/8" diameter round cathode. However, the discharge extended no farther downstream. Furthermore, the discharge became unstable when the current was increased above about 3.5 amps. It is thought that the instability arises due to lack of turbulent gas mixing near the cathode. Turbulence tends to prevent the formation of localized high discharge currents which lead to arcs. Similar results were obtained with a cathode of 1/2 inch circular cross section. A 3/8" diameter fiberglass rod placed upstream of the cathode between the cathode and anode to create added turbulence reduced the laser output power.

A double cathode consisting of two 3/8 inch diameter, hollow, water cooled copper tubes, 12 inches long was fabricated. The two parallel tubes were separated by 1.5 inches and connected electrically in parallel. The plane containing the two tubes was located parallel to the anode plane about 0.8 inches above it. As the applied current was increased up to 3 amps, the discharge was confined to the upstream tube. At 3 amps and 1050V, 105 watts of output power was obtained. Increasing the applied current made the discharge jump from the upstream tube to the downstream tube. The discharge could only be made to run from both tubes at very low gas pressure. With only the downstream tube discharge operating at 3 amps and 1040V, 55 watts of output power was obtained.

Although the visible discharge from either tube filled equivalent active volumes, the output power (for equivalent input power) for the downstream discharge was about half that obtained with the upstream discharge. This effect is not understood at this time and should be investigated further.

Adding a single wire parallel to and downstream from a single tubular cathode provided a uniform discharge the length of the anode pads. However, with 4 amps of input current and 1120V of applied voltage only 150W of output power was obtained. It is thought that the reduction of current density caused the reduction of output power.

The discharge areas of the cathode and anode were also varied in an effort to increase the laser efficiency by varying the applied current density. Extending the anode pads either laterally or longitudinally with copper tape, or reducing the anode or cathode discharge area by masking the anode or cathode with mylar tape only served to reduce the laser efficiency.

2.4.4 Final Electrode Configuration

As described previously the final cathode is a straight 5/8 inch diameter, water cooled copper tube located above the upstream end of the anode pads. There are 18 water cooled anode pads (see Section 2.3.5 for design details). Each of the 14 central anode pads is individually ballasted with a water cooled 1.3 K Ω resistor to provide uniform current distribution. Each of the two anode pads at either end of the 14 is ballasted with a water cooled 1.4 K Ω resistor to reduce the current at the ends of the cathode where arcs are most likely to form. The current through the starter wire is limited by a water cooled 2.6 K Ω resistor.

To reduce the possibility of arcing, the electrodes are all floating with respect to the laser shell.

2.4.5 Final Discharge Characteristics

The optimum output power and efficiency were obtained with the 18 anode pads configured as in Figure 21 and with the 5/8 inch diameter tubular cathode, as described in Section 2.4.4. Standard operating conditions here are 4 amps current with 1150 volts applied. Of the 4600 watts of d.c. power applied, 211 are lost in the 2600 Ω starter resistor and 941 are lost in the 68.15 Ω of equivalent ballast resistance. The starter and ballast resistors are not part of the laser head while the blower motor is and consumes 215 watts of 400 Hz power. The laser head efficiency is found to be 6% by dividing the output power (220W) by the total power to the head ($4600 + 215 - 211 - 941 = 3663W$).

An observable discontinuity in the visible emission from the discharge has been noticed between the anode and cathode running horizontally from below the cathode to the downstream end of the anode. A dark region is visible when the discharge is observed through the laser output mirror with the discharge operating without CO₂ gas present. The dark region, most likely caused by the cathode dark space, is located midway in the optical beam and could be causing the slight vertical elongation of the output beam experimentally observed (see Section 3.5). This dark region may exhibit lower gain and hence could be effecting the extraction efficiency and overall efficiency of the laser.

The anode-cathode separation has been varied as well as the location of the cathode parallel to the gas flow. The optimum separation was found to be 0.7 inches. Greater separation increases the applied voltage in such a way as to reduce the laser efficiency. Lowering the cathode further would cause it to intercept the optical beam. The location up or downstream is less critical and found to be optimum when the downstream edge of the cathode is above the upstream edge of the anode pads.

2.5 OPTICAL DESIGN

The resonant cavity optics consist of a spherical high reflectivity non-output mirror, a flat, partially transmitting output mirror, and two large, flat folding mirrors. In addition, a two element collimator can be attached to the output mirror mount to reduce the beam divergence. Within the non-output mirror mount is located a laser output power monitoring sensor. Each of these three units will be discussed in detail in the following paragraphs.

2.5.1 Resonant Cavity

A schematic of the optical resonant cavity is shown in Figure 23. The location of the anode pads and cathode is also indicated. This diagram represents the final 9-pass cavity configuration. Such a cavity configuration was chosen to provide a stable cavity, effectively use the discharge volume, and, by virtue of its length, to provide single wavelength operation without the need for an intra-cavity diffraction grating⁽³⁾. Here, the non-output mirror is a one inch diameter silicon substrate. The cavity side of the substrate has a radius of curvature, R , of 20m and has a dielectric-enhanced-metal high (>99%) reflectivity coating. The reverse side is ground flat and pressed against a flat, water cooled mounting surface.

The folding mirrors used to redirect the beam through the active discharge region are flat silicon substrates coated with the same high (>99%) reflectivity coating. They too are pressed against a water cooled mount.

The ZnSe output mirror has two flat sides, with a 4 mrad wedge between the surfaces. The side toward the laser cavity is coated with a visibly transparent coating which reflects 52% of the 10.6 μ laser beam. The reverse side has an anti-reflection coating on it at 10.6 μ and is also visibly transparent as is the ZnSe substrate. Zinc selenide was chosen for its high thermal conductivity and low absorption coefficient. The wedge angle between the two

surfaces was found to be necessary to eliminate etalon effects. With parallel surfaces, optical interference between the front and rear surface reflections would cause variations in the reflectivity of the mirror with temperature variations which in turn cause a slow jumping from one P transition to another.

Shown in view A-A of Figure 23 are the off axis mode suppression apertures. These apertures are tilted at a 10 degree angle to the folding mirrors to direct spurious reflections out of the beam downstream away from the cathode.

The optical cavity length, L_c , is 3.93m, while the active beam length in the discharge region is 2.70m. The beam radius to the $1/e^2$ intensity point at the flat output mirror, w_o , is given by the expression⁽⁴⁾

$$w_o = \left[\frac{\lambda L_c}{\pi} \left(\frac{R}{L_c} - 1 \right) \right]^{1/2}$$

With $\lambda = 10.6\mu$, $R = 20m$, and $L_c = 3.93m$, then $w_o = 0.52$ cm. The full width far field diffraction limited beam divergence angle, θ , can be found from the expression

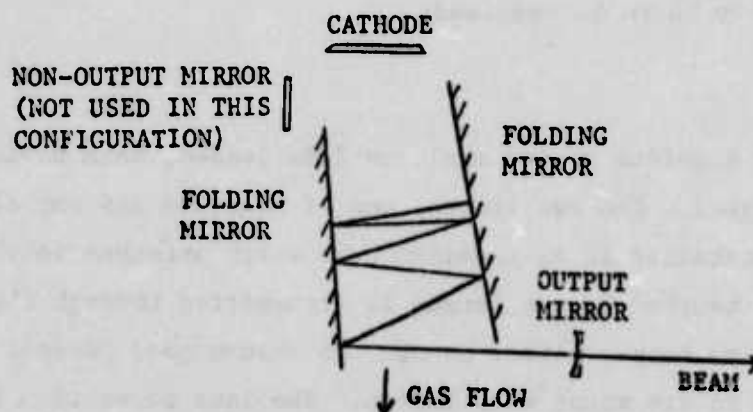
$$\theta = \frac{2\lambda}{\pi w_o}$$

to be 1.3 mrad.

Initially, the laser was designed to operate with a flat non-output mirror and a 15m radius-of-curvature output mirror. In addition, the reverse side of the output mirror was to be configured to recollimate the exiting beam. However, such an output mirror was found to be expensive and difficult to fabricate in ZnSe. After several tries, the curved output mirror was discarded in favor of a higher surface quality flat output mirror which yielded greater laser efficiency.

Several configurations of the flat folding mirrors were also tried in an attempt to optimize the laser efficiency.

By removing the tilted mode suppression plates, the flat folding mirrors could be adjusted to yield a 7 or 9 pass optical cavity. It was found that the output power was the same in either case. This result indicated that little gain was available through the downstream region of the gas. To substantiate this conclusion, the folding mirrors were aligned to concentrate the optical path away from the cathode (upstream) region of the gas as shown here.



It was found that as the beam was walked away from the cathode, the power was reduced. By exchanging the output and non-output mirrors, the beam could be walked toward the cathode. As this was done, the power increased. The conclusion is that little gain is available over the last third of the anode pads. The gain volume apparently corresponds roughly to the volume of the discharge which is visibly glowing. Attempts to extend the gain region farther downstream by varying the electrode configuration resulted in lower laser efficiency (see Section 2.4).

Non-output mirrors having a radius of curvature of 14, 20, and 30m as well as a flat mirror were used. The 20m mirror yielded the highest laser efficiency. In addition, using a flat non-output mirror, output mirrors of 52% and 60% reflectivity were tried with essentially the same output power obtained with both. Since not only the reflectivity but also the surface figure of these two curved output mirrors were different, the actual optimum reflectivity is questionable. Since the highest laser efficiency was obtained with a flat mirror of 52% reflectivity, this is the standard chosen.

Since there are four reflections from each folding mirror, a small absorption or scattering loss at the mirror greatly affects the laser efficiency. The original set of folding mirrors was measured to have a 3% loss per reflection. Analysis shows that such a loss would reduce the laser power by about 70 watts from what would be expected if the loss were 1% (as specified). Upon replacing the 3%-loss mirrors with new mirrors, an increase in output power of 20 watts from a value of 200 watts was observed. These mirrors were measured to have a loss of 2% per reflection. Mirrors of lower loss should be obtained if optimum laser efficiency is to be realized.

2.5.2 Collimator

The collimator consists of two meniscus ZnSe lenses, each having both sides anti-reflection coated. The two lenses, one of negative and one of positive focal length, are contained in an aluminum tube which attaches to the output mirror mount. Heat absorbed by the lenses is transmitted through the lens housing to the water cooled output mirror mount. To ensure good thermal transfer, each lens is sealed in its mount with indium. The lens separation is adjusted by sliding the positive lens mount within its tubular housing. A set screw clamps the sliding lens mount to the housing once it is adjusted.

The focal lengths of the two lenses were designed using basic gaussian beam propagation equations⁽⁴⁾. Using Figure 24 to define the parameters, algebraic manipulation of the basic equations yields the following expression for the focal lengths of two lenses required to expand a collimated gaussian beam of $1/e^2$ radius \bar{w}_1 to a collimated beam of radius \bar{w}_2 :

$$f_1 = \frac{d_2[w_1^2 + d_1^2 + d_1d_2] + d_2 \sqrt{w_1(d_1^2 w_2 + w_1^2 w_2 - w_1 d_2^2)}}{w_1^2 - w_1 w_2 + (d_1 + d_2)^2}$$

$$f_2 = \frac{(f_1 d_1 + f_1 d_2 - d_1 d_2)^2 + w_1^2 (f_1 - d_2)^2}{f_1^2 (d_1 + d_2) + d_1^2 d_2 - f_1 d_1 (2d_2 + d_1) - w_1^2 (f_1 - d_2)}$$

where $w = \frac{\pi \bar{w}^2}{\lambda}$.

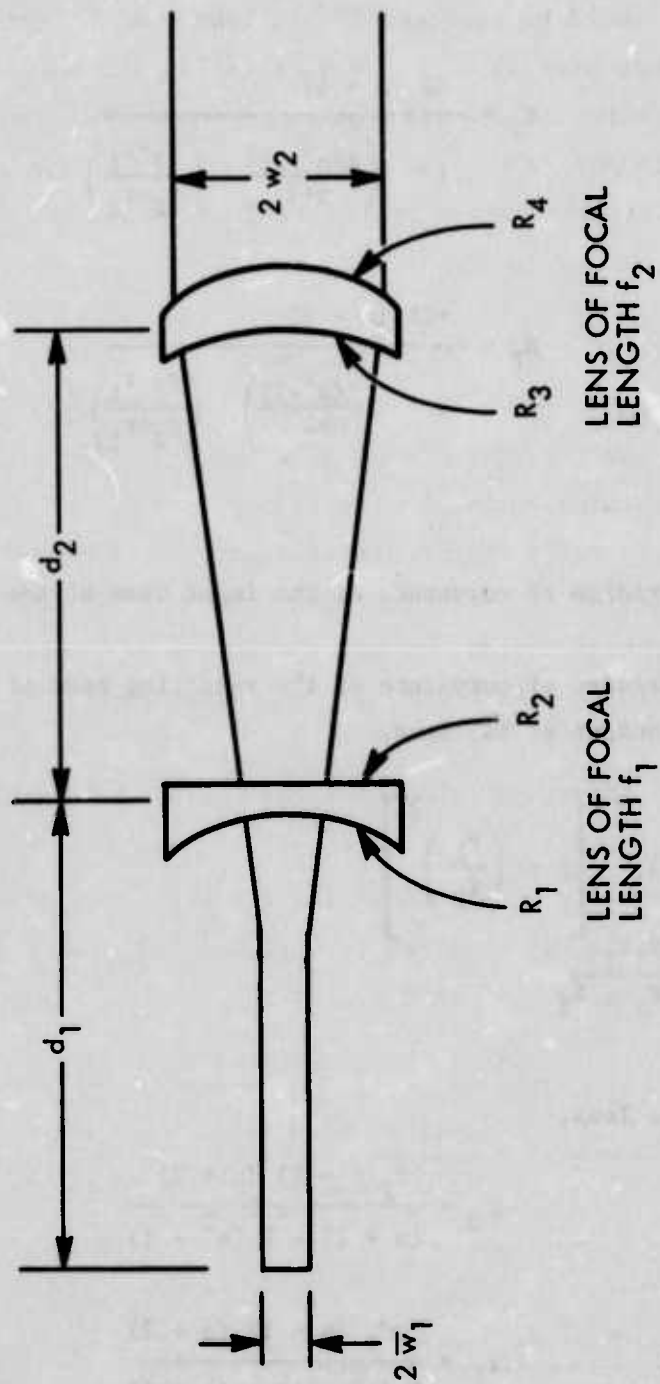


FIGURE 24 COLLIMATOR DESIGN PARAMETERS

To achieve minimum spherical aberration, the radii of curvature, R_1 (defined in Figure 24), of the two lenses of refractive index n were determined from the following relationships^(4,5): For the negative lens,

$$R_1 = \frac{2f_1(n-1)}{1 - \left(\frac{2(n^2-1)}{n+2}\right) \left(\frac{r_2-r_1}{r_2+r_1}\right)}$$

$$R_2 = \frac{-2f_1(n-1)}{1 + \left(\frac{2(n^2-1)}{n+2}\right) \left(\frac{r_2-r_1}{r_2+r_1}\right)}$$

where r_1 = radius of curvature of the input beam at the lens

r_2 = radius of curvature of the resulting beam at the output of the lens.

Here,

$$r_1 = d_1 \left[1 + \left(\frac{w_1}{d_1}\right)^2 \right]$$

$$r_2 = \frac{f_1 r_1}{r_1 - f_1}$$

For the positive lens,

$$R_3 = \frac{2f_2(n-1)(n+2)}{(n+2) - 2(n^2-1)}$$

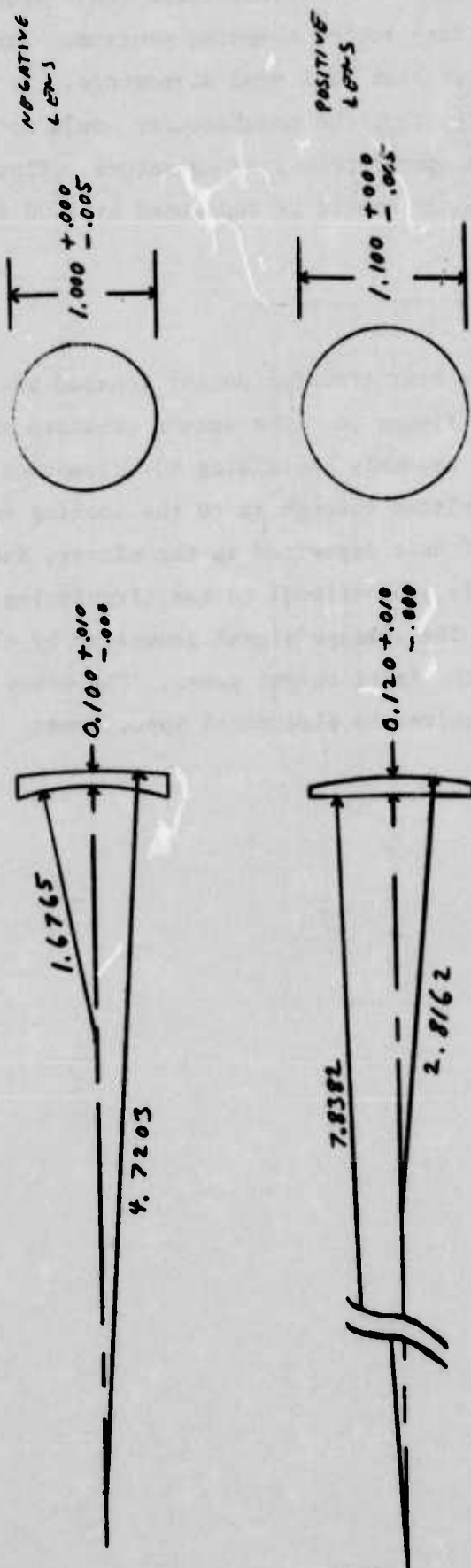
$$R_4 = \frac{-2f_2(n-1)(n+2)}{2(n^2-1) + (n+2)}$$

The lens parameters were designed with these basic equations. The design was then checked with a ray-tracing computer program. The collimator was designed to provide an output beam of 1 mrad divergence. To save cost, the lens separation was chosen so that the manufacturer would not need to make new tooling to provide the correct radii of curvature. Figure 25 details the lens design used. These lenses should be separated by 1.06 inches to provide the required collimation.

2.5.3 Power Monitor

The power monitor is a heat transfer sensor located behind the non-output laser mirror as shown in Figure 26. The sensor consists of a 1 inch diameter encapsulated thin film assembly containing 80 thermocouple pairs. It measures the heat flux transmitted through it to the cooling water from the laser mirror. The amount of heat deposited in the mirror, due to its finite absorption coefficient, is proportional to the circulating laser optical power within the laser cavity. The voltage signal generated by the detector is proportional, therefore, to the laser output power. The power monitor is compact, self-contained, and requires no electrical input power.

SPECIFICATIONS FOR GTE SYLVANIA
P.O. # 77010



SPECIFICATIONS

MATERIAL: ZINC SELENIDE (INDEX OF REFRACTION 2.40)

BULK ABSORPTION: LESS THAN 0.005 CM⁻¹ AT 10.6 MICRONS

WEDGE: LESS THAN 0.001 INCH

SURFACE FINISH: 40-10 (BOTH SIDES)

SURFACE FIGURE: LESS THAN 1 WAVELENGTH (SODIUM D)

OVER CENTRAL AREA TO WITHIN 0.050 INCH OF
EDGE (BOTH SIDES)

Figure 25 Collimator Lens Design

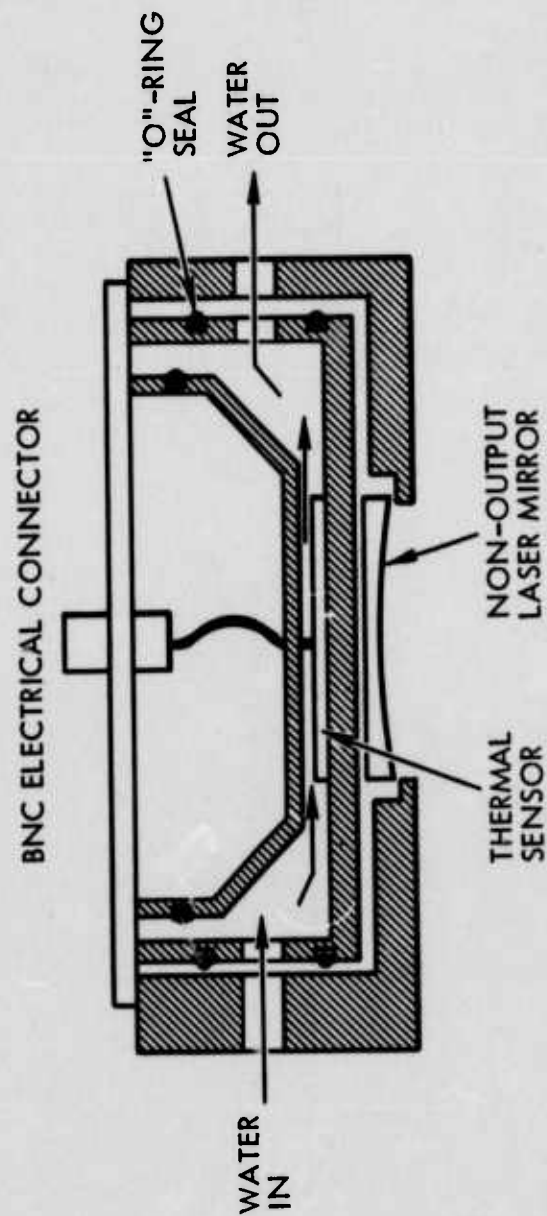


FIGURE 26 SCHEMATIC OF NON-OUTPUT MIRROR AND POWER MONITOR

SECTION III

LASER PERFORMANCE

This section details the operating characteristics of the device. The individual performance specifications listed in Table 1, Section I, will be discussed in detail in the following paragraphs. Unless otherwise noted, the performance parameters discussed were obtained using the standard gas mix of 25t He, 10t N₂, and 2.5t He with the laser drawing 4A of current.

3.1 OUTPUT POWER AND LASER HEAD EFFICIENCY

The output power, P, was measured with a Coherent Radiation Model 213 power meter located about one meter in front of the laser. The laser head efficiency, e, was calculated from the following expression

$$e = \frac{P}{VI + P_F - P_S - P_B}$$

where V = total d.c. voltage from power supply

I = total d.c. current from power supply

P_F = power applied to blower motor

P = laser output power (TEM₀₀, P(20) only)

P_S = power dissipated in 2600Ω starter resistor

P_B = power dissipated in 68.15Ω equivalent ballast resistance.

The power consumed by the blower is 215 watts.

The output power and efficiency were measured for the various cathode and anode configurations, flow vane configurations and cavity geometries described in Section 2. The results of such tests were described therein. Output power and efficiency were also measured as functions of applied current and gas mixture. The results of these tests are described here.

In general, the discharge is stable at pressures below about 42 torr. This means that the laser must be filled to a total pressure less than 42 torr to allow for the pressure rise as the gas heats during operation. The partial pressure of He is not critical; a few torr either way of the optimum pressure does not radically effect the laser power, discharge stability, or laser efficiency. The partial pressure of N_2 strongly affects discharge stability and output power. The partial pressure of CO_2 is also critical for not only power output and discharge stability, but also for laser life time. The quantitative effects of varying the gas mixture can be seen from Table II. Based on output power, efficiency, life, and discharge stability, the optimum gas mix chosen was 25t of He, 10t of N_2 , 2.5t of CO_2 .

With this gas mix, the dependence of output power and efficiency on the laser current was measured. The results are plotted in Figure 27. The normal operating current was established at 4A. The discharge becomes unstable above 5A of input current.

With the laser operating with the standard gas mix of 25:10:2.5 (He: N_2 : CO_2) and current of 4A, the output power is 220W. At 4A applied current, the power dissipated, P_g , in the starter resistor is 211 watts and in the ballast resistance, P_B , is 941 watts. The laser head efficiency, therefore, is 6% under normal operating conditions. With a clean system (well evacuated before the gas mix was put in) more power is available. Up to 300 watts have been obtained with a well cleaned system operating at 5 amps of input current.

3.2 WAVELENGTH

The laser output wavelength was measured with an Optics Technology Model 16-A grating spectrometer. As mentioned previously, when an output mirror with parallel and flat sides was used, the output was seen to jump from one P-transition wavelength to another, or to be a mixture of wavelengths, due to temperature-sensitive etalon effects in the laser output mirror. This problem was corrected by employing a wedged output mirror - one having flat sides inclined to each other at an angle of 4 mrad. With the wedged output mirror, the single wavelength of 10.59μ , corresponding to the P(20) transition, was obtained. This output wavelength does not vary with applied current or mirror alignment.

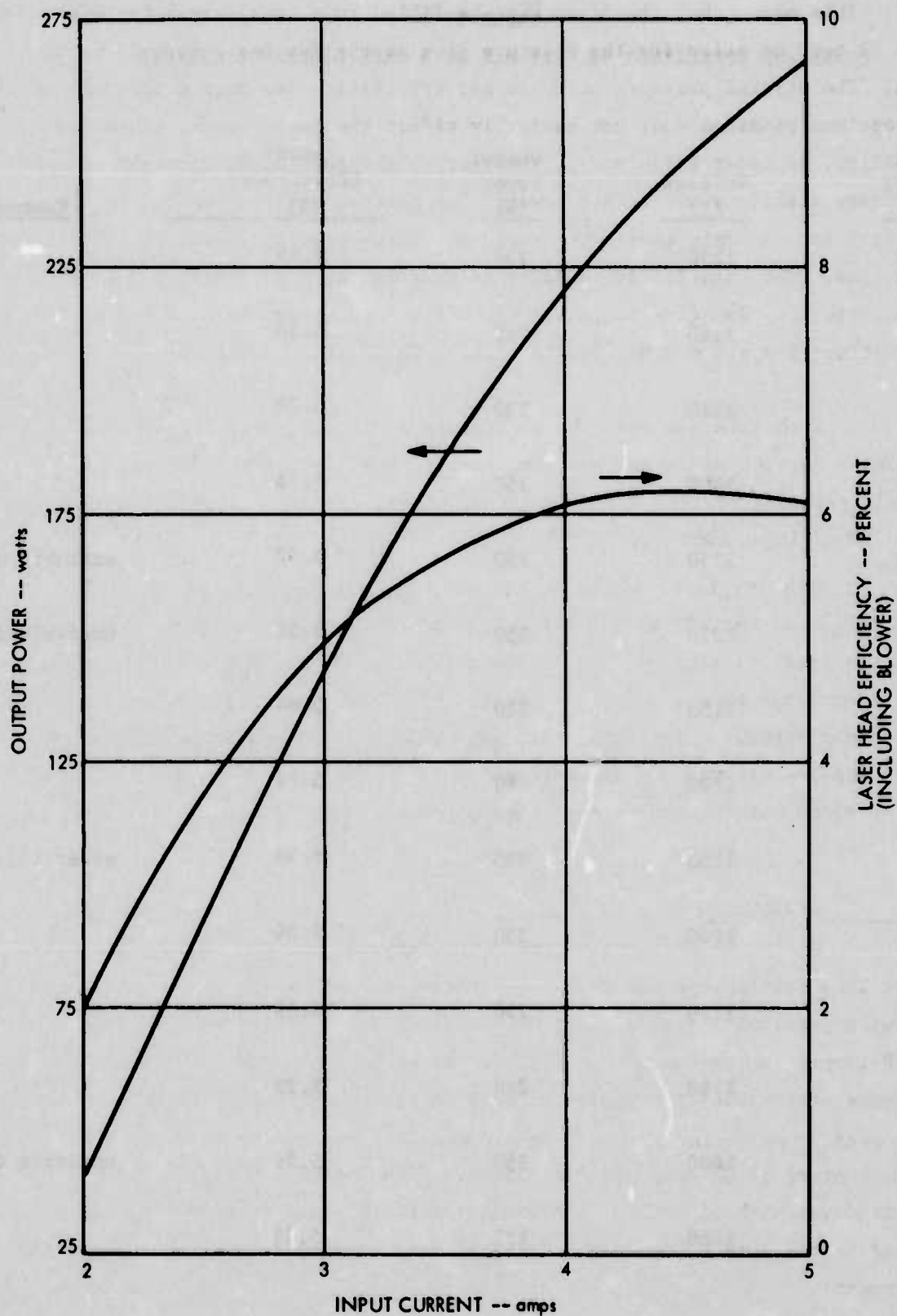


FIGURE 27 POWER AND EFFICIENCY VS INPUT CURRENT

TABLE II
POWER AND EFFICIENCY VS. GAS MIX AT 4 AMPS DISCHARGE CURRENT

<u>Gas Mix</u> <u>(He:N₂:CO₂</u> <u>(torr)</u>	<u>Voltage</u> <u>(V)</u>	<u>Output</u> <u>Power</u> <u>(W)</u>	<u>Head</u> <u>Efficiency</u> <u>(%)</u>	<u>Comments</u>
15:12.5:2	1230	230	5.68	
20:10:2	1160	210	5.58	
20:11:2	1210	230	5.79	
20:12.5:2	1300	250	5.78	
20:12.5:3	1350	250	5.52	unstable discharge
20:14:2	1350	250	5.52	unstable discharge
25:8:2	1150	210	5.64	
25:8:3	1200	220	5.61	
25:10:1	1150	200	5.36	power falls rapidly
25:10:2	1200	230	5.86	
25:10:2.5	1250	250	6.06	
25:10:3	1280	246	5.79	
25:12.5:3	1400	250	5.29	unstable discharge
30:10:2	1260	225	5.39	

3.3 TRANSVERSE MODE QUALITY

The transverse mode quality of the laser was measured by scanning a small aperture through the beam in the far field produced with a lens. A schematic of the experimental set up is shown in Figure 28. To reduce the laser power incident on the rotating aperture, the beam is reflected from a KCl wedge. The two flat surfaces of the KCl beam splitter are wedged to ensure that only one reflected beam is measured; the beam reflected from the rear surface is absorbed in a dump. A power meter behind the KCl is used to monitor laser power.

The rotating pin hole is located a distance f from the focusing lens of focal length f , so that it samples the far field pattern. Energy passing through the pin hole is collected by a lens and focused onto a fast (1 MHz) Au:Ge detector. The output of the detector is displayed on an oscilloscope triggered by a synchronizing signal from a magnetic pick-up attached to the rotating wheel containing the pin hole. To provide adequate spatial resolution, the pin hole is 0.005 inch in diameter, one tenth the diameter of the focused beam. The beam was scanned with the pin hole both in the horizontal and vertical directions.

The photograph of Figure 29 shows the output of the Au:Ge detector when no transverse mode selecting aperture is used in the laser. Here, the pin hole traversed the beam in the vertical direction. The double hump of a TEM_{10} mode can be clearly seen. The photo of Figure 30a shows the vertical beam profile when a 0.6 inch diameter mode selecting aperture is placed directly in front of the spherical non-output laser cavity mirror. The TEM_{00} mode quality is apparent. The upper trace shows the signal from the magnetic pick-up marking each rotation of the wheel. The time scale on the upper trace is 10 msec/div and on the lower trace is 50 μ sec/div. The distance from the center of the wheel to the pin hole is 2 inches.

The photo of Figure 30b corresponds to that of Figure 30a except here the pin hole scans the beam in a horizontal direction. Again, the TEM_{00} mode quality is apparent.

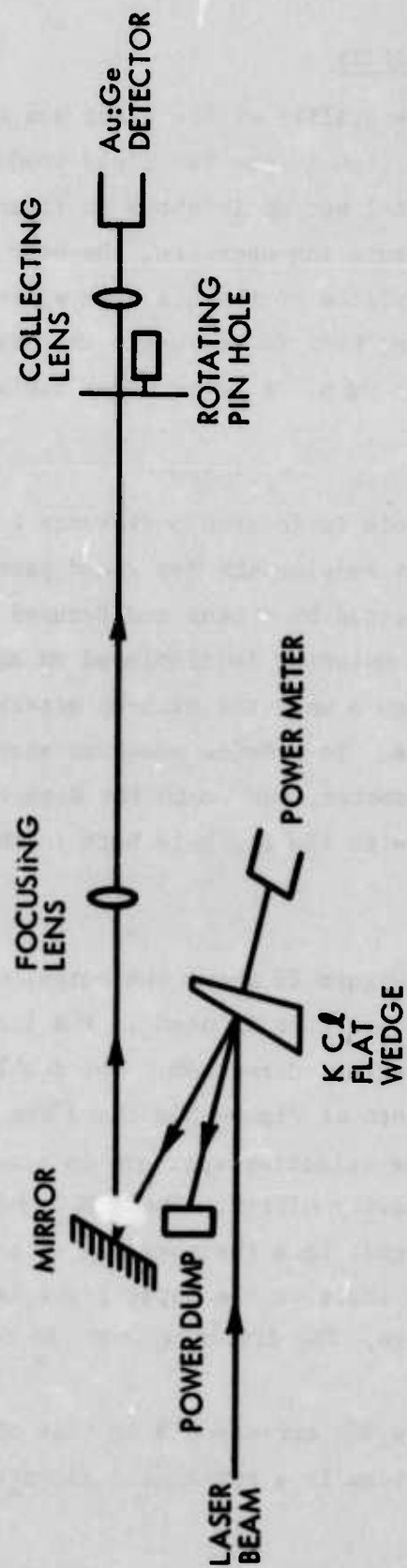


FIGURE 28 EXPERIMENTAL SET UP FOR TRANSVERSE MODE MEASUREMENT

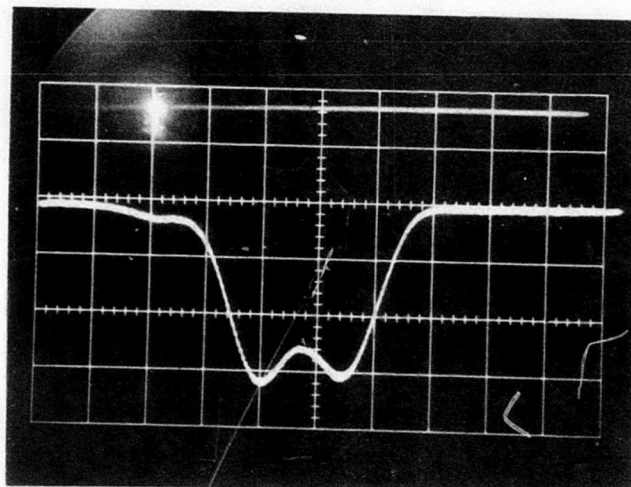
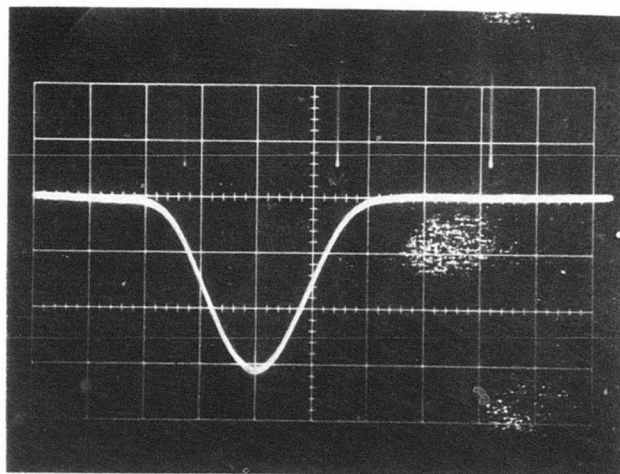
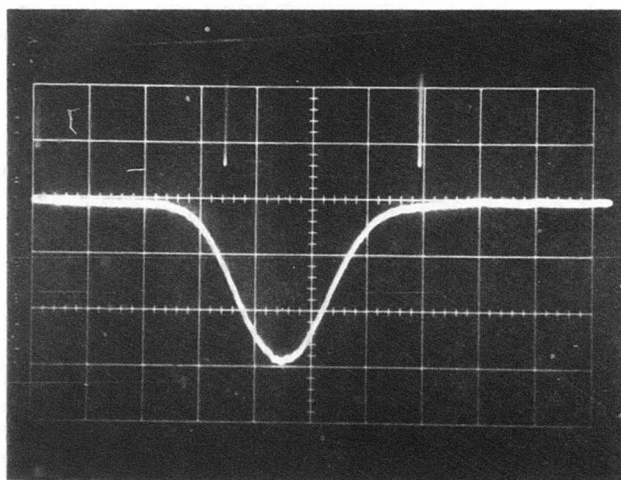


Figure 29 Beam Profile Without Aperture.
Time Scale is 50 μ sec/div.



(a) Vertical Scan



(b) Horizontal Scan

Figure 30 Beam Profile with Aperture. Top Trace: 10 msec/div.,
Bottom Trace 50 μ sec/div.

3.4 AMPLITUDE STABILITY

The laser beam amplitude stability was measured with a high-speed Au:Ge liquid nitrogen cooled detector having a frequency response of 5 Hz to 500 KHz and an oscilloscope. The experimental arrangement is shown in Figure 31. The set-up is designed to prevent any angular beam jitter from appearing as amplitude fluctuations. Accurate measurement of the basic amplitude fluctuations caused by intrinsic mechanical or thermal fluctuations of the cavity were unattainable due to the 360 Hz ripple on the three phase laboratory d.c. power supply used to operate the laser. The effect of the power supply ripple can be seen in the oscilloscope photos of Figure 32.

In Figure 32a, the upper trace shows the 360 Hz ripple from the unfiltered d.c. power supply. The ripple amplitude is about 3% of the 1150V applied to the laser. The lower trace is the laser output power as detected by the Au:Ge detector. It can be seen that the 28% ripple is correlated with the 360 Hz power supply ripple.

Figure 32b illustrates the decrease in laser beam amplitude ripple which occurs when the power supply was filtered with an available L-C network. The upper trace indicates that the filter reduces the power supply voltage ripple to about 1% of the applied 1150V. The laser beam amplitude ripple at 360 Hz is reduced to about 16%.

Although it is difficult to estimate the amount of amplitude ripple which would remain on the beam if a true d.c. power supply were used, the ripple component apparently not associated with the power supply can be estimated from Figure 32b to be about 6%.

3.5 BEAM DIVERGENCE AND ANGULAR JITTER

The full angular beam divergence is measured by the same technique used to check the transverse mode pattern (Section 3.4). The angular beam divergence θ is given by the expression

$$\theta = \frac{2\pi r t}{TF}$$

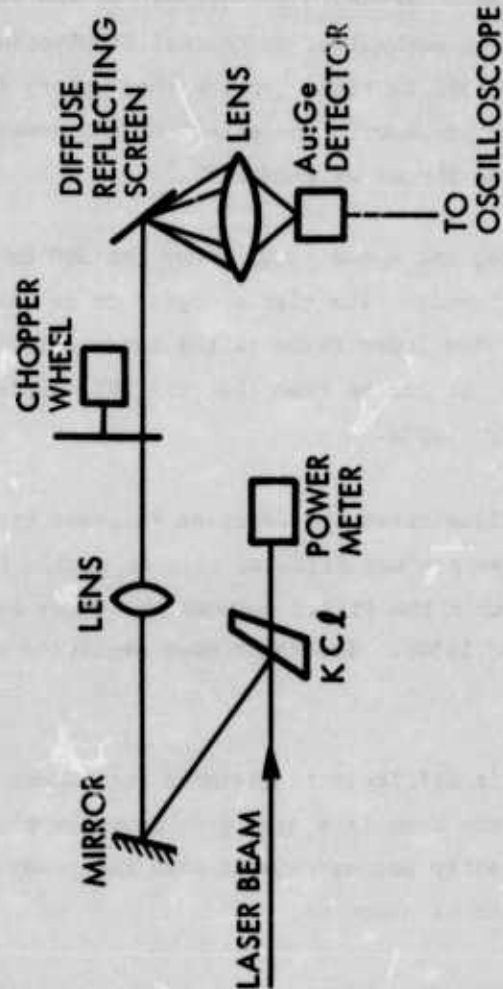
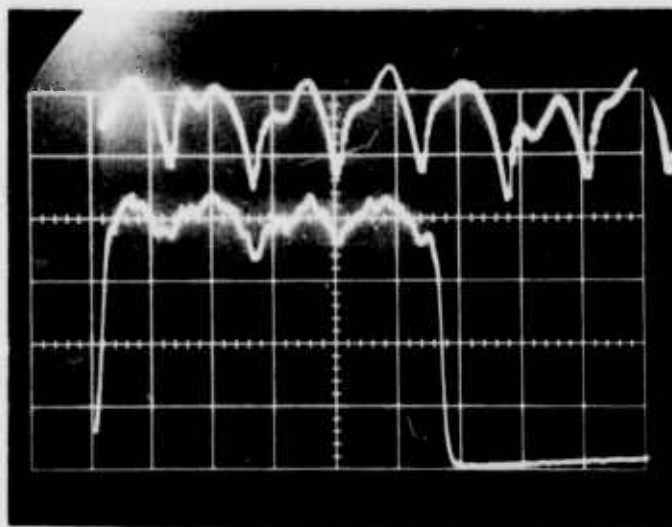
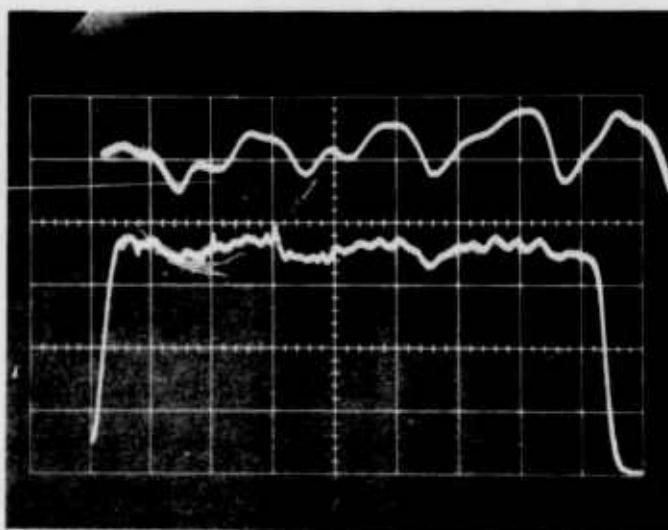


FIGURE 31 EXPERIMENTAL ARRANGEMENT FOR MEASURING AMPLITUDE STABILITY



(a) No Filter on Power Supply
 Upper Trace 20V/div, 1 msec/div
 Lower Trace 1mV/div, 1 msec/div



(b) With Filter on Power Supply
 Upper Trace 10V/div.
 Lower Trace 1 mV/div.

Figure 32 Amplitude Stability. Upper Trace is Voltage Ripple on Power Supply; Lower Trace is Laser Beam Power

where r = distance from center of wheel to pin hole
 t = width in time of beam profile as displayed on oscilloscope
between $1/e^2$ amplitude levels
 T = rotation time of wheel as measured by period of spikes
displayed on oscilloscope from magnetic pick-up
 F = focal length of focusing lens.

From oscilloscope photos such as those displayed in Figure 30, the angular beam divergence in the vertical plane with no beam collimator used was found to be 1.8 mrad. The horizontal beam divergence was found to be 1.5 mrad.

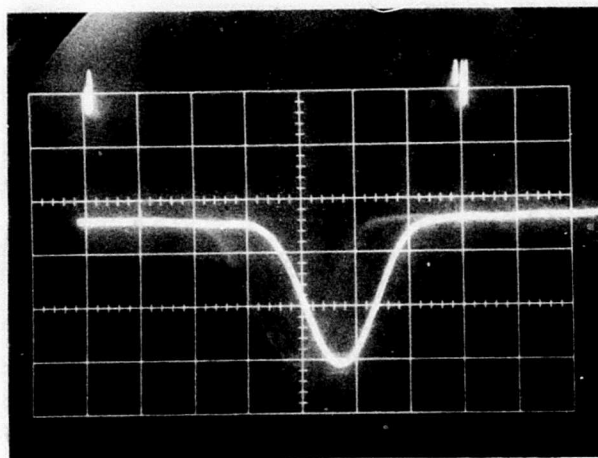
Similar photographs displaying the vertical and horizontal far field beam profiles when the collimating optics were attached to the laser are shown in Figure 33. Here the beam divergences were measured to be 1.15 mrad in the vertical direction and 0.99 mrad in the horizontal direction.

The angular deviation of the beam in time, beam jitter, was measured in vertical and horizontal directions by measuring the jitter in time of the peak of the beam profile as scanned by the pin hole and displayed on an oscilloscope. With the collimating optics attached, the vertical and horizontal jitter was measured to be less than ± 0.12 mrad.

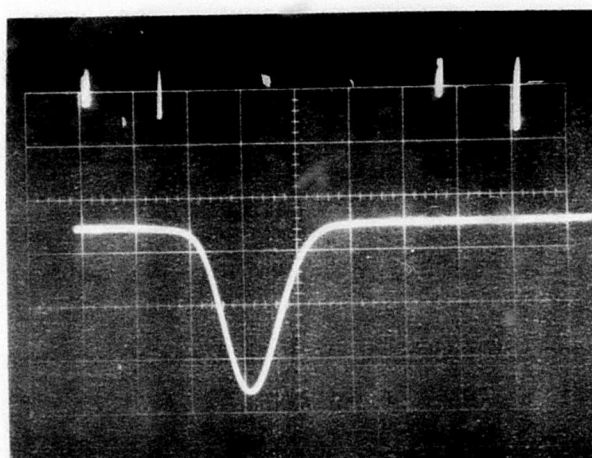
3.6 SEALED OPERATING LIFE

Two laser life timeframes were considered in designing the laser; the long-term operating time requirement of 1000 hours, and the short-term "mission time" requirement of 4 hours. There are two primary factors affecting the short-term operating lifetime of the laser, the leak rate and the gas decomposition. In the first case, air leaking into the vacuum shell contaminates the laser gas mixture and raises the gas pressure. The result is a degradation of discharge stability and reduction of laser output power.

The second power degrading mechanism is the decomposition of the laser gas mixture. The action of the discharge decomposes CO_2 molecules into CO and O_2 . The formation of oxides of the various components within the vacuum



(a) Vertical Scan



(b) Horizontal Scan

Figure 33 Beam Profile with Collimator. Time Scale:
Upper Trace 20 msec/div,
Lower Trace 200 μ sec/div.

shell tends to reduce the partial pressure of O_2 in the laser. To maintain chemical equilibrium, more CO_2 dissociates and the laser output power continuously decreases.

A solution to both these problems has conventionally been to continuously replace the gas over a period of time. This technique, however, involves the use of preset flow meters, a constant source of all gases used in the active mix, and a vacuum pump to remove gas as new gas is added. To save weight and expense and to reduce the system complexity, the laser was designed to operate in a sealed-off condition. Once filled with a lasing mix, no more gas is added to the system. Our solution to obtain the required 4-hour life was to (1) provide an essentially leak-tight vacuum shell, and (2) use a catalytic surface (the copper flow vanes) to cause the recombination of CO and O_2 back into CO_2 .⁽⁶⁾

It was found experimentally that the power monotonically decreased from 230 watts to 200 watts after 1 hour of continuous operation at 4 amps of input current, corresponding to a decrease of 13% per hour.

A power decrease of 13% per hour is greater than expected. Five possible primary causes of such a decrease are:

- (1) A greater rate of cracking of the CO_2 gas by the discharge than expected,
- (2) Contamination of the gas or electrodes by air leakage,
- (3) Contamination due to outgassing of components within the vacuum shell,
- (4) Inadequate processing of the laser prior to operation, or
- (5) Chemical reactions involving the gaseous components leaking into the system or outgassing from the system (as created by the discharge from these other components) and the electrodes or heated components within the laser vacuum shell.

To investigate the possibility that the $1.6 \mu/\text{min}$ air leak was contaminating the system and causing this power degradation, the system was filled and operated for several minutes, turned off for one hour (while sealed off),

and then turned back on again. The power at the second turn-on was identical to that of the first turn on. The conclusion is that the small leak rate does not cause the power to degrade over an hour time period at least while the laser discharge is off.

To determine the dependence of the rate of power degradation on input power, the laser was operated continuously for one hour at 3A input current. A power decrease of 13% was observed, the same as was observed with 4A of input current. We therefore conclude that the additional gas heating due to increased input power does not increase the rate of power degradation. Because the rate of power decrease was identical at 3 and 4A of current, it is felt that cracking of the CO_2 is not a primary cause of the power decrease.

It is well known that CO_2 laser lifetime is dependent on the cleanliness of the vacuum shell prior to sealed off operation. In general, repeated helium discharges and vacuum bakeouts are standard tube processing techniques which may not have been adequately performed on the 200W laser. Such processing techniques are difficult to perform on a 3 cubic foot structure, and therefore were not done on this laser head. However, since the power output does not decrease unless the laser is operated, outgassing and leakage without the presence of a discharge (or heat) does not affect the rate of laser power decrease.

It is concluded that the rate of power decrease depends on some chemically contaminating reactions between the various gases and components within the vacuum shell brought about by the action of the discharge. Therefore, unless the mechanism degrading the output power during operation can be found and corrected, the use of a gas replenishment system may be required to achieve long, continuous operation.

The primary components affecting the long-term, 1000-hours, system lifetime are the blower, cavity optics, and laser electrodes. The blower has a manufacturer-specified lifetime of 2500 hours. The mirror coatings could possibly degrade in time if the incident power density is too great. However,

manufacturers of CO₂ laser optics specify power density capabilities in excess of 300W/cm², a value some six times that occurring in the 200-watt GTL. With respect to the laser electrode design, our product GTLs have operated for over 500 hours with no degradation of the electrode structure. Because these units are water-cooled, no degradation is expected. We anticipate, then, that the components used in the laser head will allow the 1000-hour operational life requirement to be exceeded.

3.7 ENVIRONMENTAL TESTS

3.7.1 General

Selection criteria of the environmental tests that were performed on the laser head are discussed in this section. In general, the aim was to determine the suitability of the laser head for possible use in a flight test aircraft environment, while remaining within program cost and schedule constraints.

Thermal

Operational - The laser output power was measured as a function of temperature at several ambient temperatures in the operating temperature range of +40° to +100°F. No adjustments to the laser were made during the test.

Non-Operational - The laser output power was measured, with the laser temperature stabilized at ambient temperature, before and after exposure to an ambient temperature cycle of -40°F for four hours and +150°F for four hours.

Vibration and Shock

No externally applied vibration or shock tests were run on the laser head. This decision was based on the assumption that the laser head can be rigidly mounted on a platform shock-and vibrationally-isolated from the aircraft.

Humidity

No test of laser performance in a humid atmosphere was performed, because a) the materials exposed to the ambient air are by design not sensitive to water or water vapor exposure, b) the high voltage connections are

either potted or are in standard connectors, and c) the power supply is not included with the head.

Pressure

A pressure difference across the vacuum shell has the potential for distortion of the shell. This distortion could couple into the mirrors, causing optical misalignment. The laser output beam power and pointing direction could, therefore, change as a result of a change in ambient pressure. Distortion of the cavity was measured as the laser head internal pressure was varied from 40 torr to 280 torr (corresponding to decreasing the external pressure from that at sea level to that at 10,000 feet).

Maximum pressure differential, and therefore maximum pressure induced stresses, occur while the laser head is filled to operating pressure and is at sea level. The flight test ambient pressure - induced mechanical stresses, therefore, are lower than those the laser head has already withstood numerous times.

3.7.2 Temperature

For the operational tests, the laser head was placed inside an insulated box along with a heater and, for the cold temperatures, dry ice. The laser output power was found to vary by 30% as the ambient temperature was varied from 40°F to 100°F. The variation in output power was found to be caused by misalignment of the cavity mirrors due to differential expansion of the support invar rods. If large, non-uniform temperature variations are expected in use, it may be necessary to control the temperature of the four individual invar cavity support rods. For example, the rods may be replaced with hollow tubes with temperature regulated coolant passed through them at very low flow rates.

To test laser integrity at the possible storage temperatures, the laser head was first placed in a temperature chamber at 150°F for 4 hours. The chamber temperature was then lowered to room temperature for several hours. The temperature was then further lowered to -40°F and held there for 4 hours. The laser was then checked for leaks (at room temperature). Three leaks were found: one

between each epoxy-plastic interface sealing the cathode and starter wires as they enter the laser shell, and one at the epoxy-aluminum interface sealing the cathode water lead as it enters the laser shell. In all three locations, seals can be designed using "O" rings instead of epoxy.

3.7.3 Ambient Pressure

To measure the distortion of the cavity structure occurring upon ambient pressure changes, two quartz flats were mounted to the top of the cavity support plates. The two flats were oriented so that they formed a flat-flat interferometer with a spacing equal to the separation of the cavity support plates from one another. A collimated He-Ne laser was used as the source beam for the interferometer. As the gas pressure inside the laser shell was varied from vacuum to atmospheric pressure, the distortion of the end plates could be observed as a variation in the fringe pattern produced by the He-Ne laser beam passing through the quartz interferometer.

The change in relative angle, $\Delta\theta$, between the two cavity support plates for a given pressure change is given by

$$\Delta\theta = \Delta N \frac{\lambda}{2d}$$

where ΔN = change in the total number of fringes in a given area of the interference pattern

d = quartz plate separation

λ = He-Ne laser wavelength.

The change in separation, Δt , of the two quartz plates (mounted to the top, center of the cavity support plates) is given by

$$\Delta t = \frac{n\lambda}{2}$$

where n = number of fringes passing a fixed point in the interference pattern.

From these expressions, it was found that $\Delta\theta = 0.32$ mrad and $\Delta t = 0.0034$ inch for a change of pressure equal to an atmosphere. This large distortion would cause a large variation in output power with a pressure variation corresponding to a few thousand feet of altitude change if the laser optics were not realigned.

To correct this problem, thicker optical support plates and heavier invar cavity support rods would be needed.

3.8 SUMMARY AND CONCLUSIONS

A compact, lightweight, 200 watt (cw, TEM₀₀, single P-line), amplitude stable CO₂ laser head has been designed, fabricated, and tested. As indicated by Table I, all performance specifications have been essentially met with the exceptions of the sealed-off operating time and the laser head efficiency. Consistent with the program goals, a 200 watt laser head has been developed that can provide the basis of an airworthy system.

Without further investigations being made to allow the sealed-off continuous operating life to be extended, providing the laser head with an automatic gas replenishment system would allow the laser to operate continuously almost indefinitely.

The laser efficiency could be increased by further optimizing the output mirror transmission, reducing the absorption and scattering losses of the cavity mirrors, further cooling the circulating laser gas, increasing the blower speed, possibly reducing the cavity from nine to seven passes, or possibly redesigning the electrode structures.

The only other problem disclosed by testing the device was the instability of the cavity structure during ambient pressure variations. Minor modifications to stiffen the cavity structure would correct this problem.

SECTION IV

CONCEPTUAL AIRWORTHY DESIGN

One of the major objectives of this program was to furnish a conceptual design for a complete laser system that incorporates and is compatible with the laser head developed during the program. The laser head design should outline the laser's growth potential for applications into a ruggedized, operational airborne system.

The airborne laser system would consist of five basic units:

- 1) Laser head,
- 2) Power supply,
- 3) Cooling system
- 4) Gas fill system, and
- 5) Control/monitor panel.

The following paragraphs will discuss the design of each unit.

4.1 LASER HEAD

The laser head, consisting of an electrode structure, internal heat exchanger, blower, optical cavity, collimator, power monitor, and vacuum shell, would be designed as described in Section 2 and 3 above. The following modifications would be made to ensure an airworthy design.

First, the cavity support plates should be stiffened by replacing the aluminum with steel or designing a ribbed structure. The invar support rods should also be made larger in diameter to stiffen the optical structure. With such a structure, the optical cavity alignment would no longer change with ambient pressure (altitude) changes. Since the laser head is well under the allowable weight, heavier cavity structure would present no weight problem.

Another way to handle this problem is to include the cavity support structure within the vacuum shell. Less convenient mirror adjustment, an added beam output window, significant redesign of the head, and difficulty in providing for resonator cavity alignment to an external reference line, would be the costs.

Second, the viewing port and gas flow control channel, both made of Pyrex, should be securely clamped to survive vibration. The plates are made of glass to allow the discharge and electrodes to be observed. Although it is not absolutely necessary to observe the discharge region so that the glass could be replaced with high temperature ceramic, the advantages offered by glass recommends its use.

The third modification involves clamping the cavity adjustment screws. Once the cavity is aligned, the adjustment screws should be designed to be locked in place to prevent cavity misalignment during vibration.

Another modification would be to weld the gas flow vanes in place within the laser end bells. This can be done since their location has now been determined. Likewise, the cathode need no longer be adjustable. A modification of the cathode mount would eliminate the epoxy seals.

In an airborne system, the optical cavity should be mounted to an optical bench isolated from the laser vacuum shell. This would ensure that the output beam direction would remain fixed regardless of flight environmental conditions.

The epoxy seals at the cathode and at the electrical feedthroughs should be replaced with "O"-ring seals to eliminate the occurrence of leaks at these seals during thermal stress.

Because of platform vibration, the Wallace-Tiernan pressure gauge would have to be vibrationally mounted or eliminated. All gas and vacuum valves would have to be rigidly mounted.

These relatively minor modifications would make the existing laser head airworthy while increasing the weight by about 25 pounds.

4.2 POWER SUPPLY

The power supply must be highly filtered and capable of producing 4.5 amps of d.c. current at about 1400 volts. The supply should be current regulated to provide a constant current since gas pressure and composition change with temperature leading to discharge impedance variations during operation.

From measurements of the amplitude stability of laser output power and power supply voltage performed on this program, it is estimated that the power supply ripple should not exceed 0.05%.

The power supply, including the ballast, can be very simple and efficient, consisting of an ac three-phase controller, a three-phase step-up transformer, a three-phase full wave rectifier bridge, an L-C filter network, and a current control circuit.

The input VA required for such a dc discharge source (including ballast) may be determined below:

Normal discharge including	
68 Ω ballast (4.0A @ 1150V)	4600W
L-C Filter Loss (4%)	184W
3 ϕ Full Wave Rectifier Loss (2%)	96
3 ϕ Transformer Loss (1.5%)	73
3 ϕ Controller Loss (3%)	149
Line Power Factor (0.955)	240
Total Input VA	5342W

The dc discharge source is not complicated in design and does not require a substantial design effort. With the exception of the step-up transformer, the components are readily available, standardized parts (filter capacitors, rectifiers, etc.). Development will be needed, however, to minimize the overall size and weight of the power supply.

The efficiency of the supply depends in part on the actual value of the current limiting ballast resistors connected to each of the 18 anode pads forming the laser discharge anode. The minimum value of these resistors needed to maintain a stable discharge was not determined during this program.

The power supply will require EMI filtering primarily at the input to the power supply to meet requirements of MIL-STD-461. These four filters will weigh approximately a total of 40 pounds and require 0.4 ft.³ of volume.

To prevent arcing in the discharge during turn-on, it is necessary to apply voltage to the head slowly until the glow discharge is formed between cathode and anode. With fast turn-on circuitry, pushing an "on" button would automatically apply voltage to the laser and slowly raise it (over a few seconds) until the current reached a preset value. Such a system is used in the Model 971 product GTL.

For airborne operation the power supply should operate from a 3 phase, 208 volt, 400 Hz source. It is estimated that such a supply would weigh about 120 pounds and would have a volume of 3.0 feet³ excluding the 40 pounds and 0.4 ft.³ of the EMI filters.

4.3 COOLING SYSTEM

The water flow rate required to cool the internal laser heat exchanger, laser electrodes, and optical structure is 2 gal/min. To survive the low temperature extremes, anti-freeze, compatible with the coolant lines, would have to be added.

If the power monitor unit attached to the rear laser mirror is used, it must be cooled with coolant whose temperature is not affected by the temperature of the laser head.

The external heat exchanger must be capable of removing about 5 KW of power generated by the laser and ballast resistors. A simple ram air heat exchanger could readily handle this load.

Coolant lines would then run from the coolant circulator, to the laser head (where it first cools the power monitor), then to the ram-air heat exchanger, and back to the circulator.

The coolant circulator would consist of a pump, reservoir, heater, and flow rate interlock. The pump should provide a 2 gal/min flow rate, and the laser power supply should be made inoperable if the flow rate falls much below this. Consuming 300 watts of power, a 1/3 h.p. motor would be sufficient. The estimated weight of the coolant circulation unit (excluding ram air heat exchanger) is 70 pounds. The volume is estimated to be 3 feet³.

4.4 GAS FILL SYSTEM

Two modes of laser operation can be considered: the sealed off mode or the gas replenishment mode. It has been found experimentally that the sealed-off, continuously operating, life is limited probably by contaminating chemical reactions at the electrodes. When operating sealed off, the laser is first evacuated, then filled to the proper pressure with the proper gas mix, and then sealed off, i.e., the vacuum pump and gas bottles can be removed. This is the simplest system but, unless the cause of the power degradation can be found and corrected, also results in a slow power roll-off with operating time.

To extend the operating time indefinitely, a constant gas replenishment system would be required. Here, gas from a premixed gas bottle is continuously introduced into the system. An active pressure sensor then senses when the pressure increases beyond a fixed value, and activates a solenoid valve connecting the laser vacuum shell with a vacuum pump. When the pressure is reduced to some preset level, the valve closes. Depending on the gas replenishment rates actually required to achieve a given life, the vacuum pump may be replaced by an evacuated bottle.

At a gas replenishment rate equal to that of the Model 971 GTL (two feet³/hour into 26 feet³ of volume) then a 4 inch diameter x 12 inch bottle filled with 50 atmosphere liters of premixed gas and weighing two pounds would be required to achieve about 30 hours of continuous operation in the smaller

200 watt laser. The vacuum pump would consume 375 watts of power and weigh 50 pounds. The active pressure gauge and solenoid valve would weigh about 5 pounds. Because maintenance on the ground is possible, a technique which uses a much lighter, smaller pump to maintain the laser pressure at ~40t might be used. The full evacuation would only be performed with the "good" ground based pump.

It must be emphasized that the added weight and complexity of such a gas replenishment system might be avoided if 1) the mechanism causing the sealed-off operating life to be limited were found and corrected, and 2) the actual operating scenario (on time vs off time) were established.

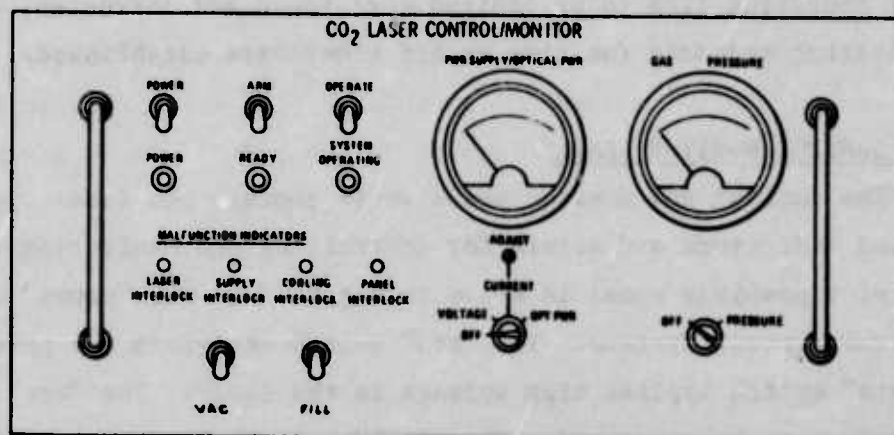
4.5 CONTROL/MONITOR PANEL

The control and monitor panel would contain the laser operating switches and indicators and meters for controlling and monitoring the system. A drawing of a possible panel is shown in Figure 34. The "power" switch energizes the control systems. The "arm" switch energizes the power supply. The "operate" switch applies high voltage to the laser. The "vac" switch allows the system to be evacuated. The "fill" switch allows gas to enter the system to a pressure indicated on the "gas pressure" meter. The operating current is set with a screw driver adjustment. Applied voltage, current, or optical output power (derived from the power monitor at the rear of the laser head) can be read on a meter. Various interlocks protect the system and operator.

Such a panel may weight 30 pounds and require about 0.6 feet³.

4.6 VOLUME REDUCTION

It is felt that it is not an easy task to modify this basic laser system design to reduce the volume to the design goal of 1 foot³ and the weight to 100 pounds. Reducing the laser head alone to 1 foot³ would be a formidable task: Some size reduction could be obtained if the laser could be operated at higher gas pressure and higher gas flow velocities. (See Section V.) In this case, the optical gain path length could be reduced. However, the relatively fixed sizes of the required internal heat exchanger



Figur. 34 Control/Monitor Panel

and blower probably limit the size reduction possible. It is felt that this basic design cannot produce equivalent performance in a substantially reduced volume. The key to reducing the size is to increase the laser efficiency because this would enable the size of the discharge volume and the internal heat exchanger to be reduced. Research, therefore, should be conducted with this goal in mind. Such research should center on increasing the flow velocity, and gas pressure, and investigating various other electrode configurations.

4.7 SUMMARY

The conceptual design for an airworthy system consists of 1) relatively minor modifications to the basic laser head design developed on this program, and 2) auxiliary electronic and coolant units with function, weight, volume, and power requirements estimated from our experience with other airworthy gas transport lasers. A summary of the system design parameters is given in Table III.

TABLE III
AIRWORTHY LASER DESIGN

<u>Component</u>	<u>Input Power (w)</u>	<u>Weight (lbs)</u>	<u>Volume (ft.³)</u>
Head		125	3.0
Blower	215		
Power Supply			
(4A @ 1150V output)	5342	120	3.0
EMI Filters		40	0.4
Cooling System	300	70	3.0
Gas Replenishment System	375	60	1.3
(>30 hrs. continuous operation)			
Control/Monitor Panel	50	30	0.6
TOTAL	6282W	445 lbs.	11.3 ft. ³

SECTION V

CONCLUSIONS AND RECOMMENDATIONS

The basic objectives of the program have been satisfied. A compact, lightweight, 200 watt, TEM₀₀, single P-line, amplitude stable CO₂ laser head has been designed, constructed, and tested. A conceptual design for an air-worthy system has been completed which is based on the system developed during the program.

It is recommended that the following modifications and investigations be made to improve the laser performance capability.

First, because it is very desirable to operate in the sealed off mode, an investigation to determine the cause of power degradation with sealed off operating time is recommended. Such an investigation should include a study of the effect that the leak rate, copper catalyst, and gas additives (H₂O, Xe) have on operating lifetime. Analysis of the gas composition during operation and the factors such as temperature, pressure, initial gas mix, amount and temperature of catalyst, leak rate, etc., which affect the composition should be undertaken.

If the rate of power degradation cannot be appreciably reduced, then corrective action through the use of a gas replenishment system should be investigated. Part of this investigation should include determining the minimum rate of replenishment required.

Several investigations should also be undertaken to increase the laser overall efficiency. First, the optical gain at different locations in the discharge region should be studied in order to understand the results of the double cathode experiment discussed in Section 2.4 and the optical cavity experiments discussed in Section 2.5.1. If it is found that gain is low downstream due to poor electrical excitation, then other electrode configurations should be investigated. Relatively minor modifications to the existing electrode configuration could result in a field being applied along, instead of transverse to, the

gas flow velocity. Such a discharge may provide a more uniform volumetric excitation of the gas.

Discharges which are more longitudinal (higher voltage, lower current) rather than transverse (lower voltage, higher current) should have higher efficiency because the fixed anode-cathode losses, which are more important in these small systems, are reduced. For instance, with 330V of combined anode-cathode fall voltage and a current of 4A, 1320 watts of power are lost to the anode and cathode. This is 29% of the total power applied to the discharge. Changing the electrode geometry to excite the same gas volume but to also increase the operating voltage and reduce the operating current would reduce the power lost to the electrodes.

Other electrode configurations should be investigated, especially in these small systems, to reduce the effect of discharge non-uniformities near the cathode. As noted in Section 2.4.5, a visibly darkened region associated with the cathode is located in the region transversed by the laser beam. Reconfiguring the electrodes to move this dark region out of the beam may increase the laser efficiency.

Other parameters which should be investigated further in an effort to improve the overall laser efficiency are the absorption and scattering losses of the laser mirrors and the transmission of the output mirror. The minimum value of ballast resistance required to maintain a stable discharge should also be determined.

To increase the laser power, investigations of electrode configurations, rapid double pulse discharge techniques, and discharge pre-ionization techniques should be undertaken to allow a stable discharge to be operated at increased gas pressure. Along these same lines, methods for increasing the gas flow velocity (and therefore output power) should be investigated.

These investigations are particularly important, in that the results determine the feasibility of reducing the size of the head.

Finally, to increase the beam stability during ambient pressure changes, the resonant cavity structure should be stiffened.

To summarize, a basic 200 watt TEM₀₀ mode cw CO₂ laser has been developed. The knowledge gained from this system allows recommendations to be made for further investigations which would result in even higher power, efficiency, and stability.

SECTION VI

REFERENCES

1. A. J. DeMaria, Proc. IEEE, 61, 731 (June 1973).
2. Unpublished research experiments performed by R. Kirk and J. Foster
3. M. Sasnett, R. Reynolds, IEEE J. Quant. Elec., QE-7, 372 (July 1971).
4. H. Kogelnik, T. Li, Proc. IEEE, 54, 1312 (Oct. 1966).
5. F. Jenkins, H. White, "Fundamentals of Optics", McGraw-Hill, N.Y., 1957.
6. U. Hochuli, T. Sciacca, IEEE J. Quant. Elec., QE-10, 239 (Feb. 1974).

UNCLASSIFIED

AD B00 4286

AUTHORITY:

AFUWL

1cc, 19 OCT 81



UNCLASSIFIED